
Masters Theses

Student Theses and Dissertations

Fall 2015

Synthesis of different sizes & functions nanoparticles

Jiaming Geng

Follow this and additional works at: https://scholarsmine.mst.edu/masters_theses



Part of the [Chemistry Commons](#), and the [Petroleum Engineering Commons](#)

Department:

Recommended Citation

Geng, Jiaming, "Synthesis of different sizes & functions nanoparticles" (2015). *Masters Theses*. 7464.
https://scholarsmine.mst.edu/masters_theses/7464

This thesis is brought to you by Scholars' Mine, a service of the Missouri S&T Library and Learning Resources. This work is protected by U. S. Copyright Law. Unauthorized use including reproduction for redistribution requires the permission of the copyright holder. For more information, please contact scholarsmine@mst.edu.

SYNTHESIS OF DIFFERENT SIZES & FUNCTIONS NANOPARTICLES

by

JIAMING GENG

A THESIS

Presented to the Faculty of the Graduate School of the
MISSOURI UNIVERSITY OF SCIENCE AND TECHNOLOGY

In Partial Fulfillment of the Requirements for the Degree

MASTER OF SCIENCE
in
PETROLEUM ENGINEERING

2015

Approved by
Dr. Baojun Bai, Advisor
Dr. Schuman P. Thomas, co-advisor
Dr. Ralph Flori

© 2015
JIAMING GENG
All Rights Reserved

ABSTRACT

Nanogels, whose size range from 1 to 100nm, have been interested in many research areas: cosmetics, pharmaceuticals, catalysts, photochemistry, and in optical switches or sensors. In Petroleum Engineering area, nanogels can be used as conformance control agent and emulsion stabilizer. And after grafting functional groups or hybrid, nanogels can be used as tracer for the visual modeling.

Though nanoparticles have been studied for more than 20 years, few of them are about nanogels. In the thesis, stirring rate, surfactant type and concentration were found have a large impact on the synthesis of nanogels. And cationic nanogels have salt and acid resistant properties.

In the thesis, the most used methods for synthesizing small size particles is reviewed. The experiments section covers three parts: a) microemulsion preparation, b) cationic nanoparticles synthesis and evaluation, c) nanoparticle size control. In microemulsion preparation part, optimum surfactants ratio of Span80 to Tween60 was given. In cationic nanoparticles synthesis and evaluation part, nanoparticles of different cationic degree were synthesized via suspension polymerization. And after introducing cationic groups to it, nanoparticles can have acid and salt resistant properties. In size control part, stirring rate, type and concentration of surfactants all affect the morphology and size of nanogels.

ACKNOWLEDGEMENTS

First and foremost I want to express my deepest gratitude to my advisor, Dr. Baojun Bai, for his guidance, time and funding to provide me with an outstanding atmosphere for doing research. It has been an honor to be his student.

Also I would like to thank my co-advisor, Dr. Schuman Thomas, for his guidance and valuable discussions during my research. The extracurricular talks ignited my mind.

I would also like to thank Dr. Flori for his help during well testing class.

I would like to give my sincere gratitude to Zun Chen, Jingyang Pu, Songyuan Liu and Dr. Farag for their help during my lab setup. Also, I would like to thank all of my labmates: Danlu Zhang, Yifu Long, Yizhou Wu, Dr. Wang, Yue Qiu, Na Zhang, Yandong Zhang, Ze Wang, Haifeng Ding, Abdulmohsin Imqam, and Alhuraishawy, Ali for their help and teamwork.

I would also like to thank my parents for their encouragements and care.

TABLE OF CONTENTS

| | Page |
|--|------|
| ABSTRACT | iii |
| ACKNOWLEDGEMENTS | iv |
| LIST OF ILLUSTRATIONS | vii |
| LIST OF TABLES | iix |
| NOMENCLATURE | x |
| SECTION | |
| 1 INTRODUCTION | 1 |
| 2 LITERATURE REVIEW | 4 |
| 2.1 GENERAL FEATURES OF EMULSION & SUSPENSION POLYMERIZATION PROCESS..... | 4 |
| 2.1.1 Compositions of Polymerization. | 4 |
| 2.1.2 Mechanism of Polymerization..... | 5 |
| 2.2 SUSPENSION POLYMERIZATION..... | 9 |
| 2.2.1 Process Description. | 9 |
| 2.2.2 Size Control & Morphology..... | 12 |
| 2.3 EMULSION POLYMERIZATION | 13 |
| 2.3.1 Process Description. | 13 |
| 2.3.2 Conventional Emulsion Polymerization..... | 13 |
| 2.3.3 Soap-free Emulsion Polymerization..... | 15 |
| 2.3.4 Size Control & Morphology..... | 18 |
| 2.4 OTHER TECHNIQUES..... | 18 |
| 3 PREPARATION OF MICROEMULSION | 22 |
| 3.1 MATERIALS | 22 |
| 3.2 SURFACTANT RATIO SELECTION | 22 |
| 3.3 MICROEMULSION DETERMINATION | 25 |
| 3.4 PSEUDO-TERNARY PHASE DIAGRAM..... | 27 |
| 4 SYNTHESIS & EVALUATION OF CATIONIC NANOPARTICLES..... | 28 |

| | | |
|-------|---|----|
| 4.1 | MATERIALS | 28 |
| 4.2 | SYNTHESIS OF CATIONIC NANOPARTICLES | 28 |
| 4.3 | EVALUATION OF CATIONIC NANOPARTICLES | 29 |
| 4.3.1 | Morphology of Cationic Nanoparticles..... | 29 |
| 4.3.2 | Effect of Cationic Degree of Nanoparticles..... | 32 |
| 4.3.3 | Effect of Salinity on Nanoparticles..... | 38 |
| 4.3.4 | Effect of PH on Nanoparticles..... | 41 |
| 5 | SIZE CONTROL OF NANOPARTICLES | 44 |
| 5.1 | MATERIALS | 44 |
| 5.2 | DIFFERENT FACTORS EFFECT ON PARTICLE SIZE..... | 44 |
| 6 | CONCLUSION..... | 56 |
| | BIBLIOGRAPHY | 57 |
| | VITA | 63 |

LIST OF ILLUSTRATIONS

| | Page |
|---|------|
| Figure 2.1 SEM photo of polymer samples produced by suspension polymerization. .. | 14 |
| Figure 2.2 Mechanism for the preparation of microgel particles by surfactant-free emulsion polymerization. The steps shown are initiator decomposition (a), initiation (b), propagation (c), particle nucleation (d), particle aggregation (e), particle growth (in a poor solvent) (f), and particle swelling in a good solvent (g)..... | 16 |
| Figure 2.3 SEM photo of polystyrene particles synthesized in scCO ₂ by dispersion polymerization. | 19 |
| Figure 3.1 Boiling points of different n-alkane (from C ₁ to C ₁₆)..... | 23 |
| Figure 3.2 Variation of electrical conductivity of emulsion as a function of aqueous solution content..... | 26 |
| Figure 3.3 Experiment design for Pseudo-ternary phase diagram. | 27 |
| Figure 4.1 Morphology of cationic nanoparticles swelled in 1wt.% NaCl (ESEM)..... | 30 |
| Figure 4.2 Morphology of cationic nanoparticles (SEM). | 31 |
| Figure 4.3 Nanoparticles in the fractures of a powder. | 31 |
| Figure 4.4 The average diameter of fully swelled nanoparticles in deionized water (black column) and 1wt.% NaCl solution (red column). | 32 |
| Figure 4.5 Dispersion viscosity of 0% cationic degree nanoparticles (concentration from 0.1 to 1wt.%). | 34 |
| Figure 4.6 Dispersion viscosity of 5% cationic degree nanoparticles (concentration from 0.1 to 1wt.%). | 34 |
| Figure 4.7 Dispersion viscosity of 10% cationic degree nanoparticles (concentration from 0.1 to 1wt.%). | 35 |
| Figure 4.8 Dispersion viscosity of 15% cationic degree nanoparticles (concentration from 0.1 to 1wt.%). | 35 |
| Figure 4.9 Infinite shear viscosity of cationic nanoparticles..... | 36 |

| | | |
|-------------|---|----|
| Figure 4.10 | Intrinsic viscosity of cationic nanopartilces (● intrinsic viscosity by Kraemer Equation, ■ intrinsic viscosity by Huggins Equation). | 37 |
| Figure 4.11 | Measured equilibrium swelling diameter of cationic nanoparticle (15% cationic degree) in different brine solution. | 39 |
| Figure 4.12 | The infinite shear viscosity of nanoparticle dispersion..... | 39 |
| Figure 4.13 | Zeta potential of 15% cationic degree nanoparticles as a function to the surrounding solution salt concentration (from 0 to 2%). | 40 |
| Figure 4.14 | Equilibrium swelling ratio of 15% cationic degree hydrogel (PAM-co-AETAC) and PAM in different pH value solutions (from 1.0 to 7.0). | 41 |
| Figure 5.1 | Structures of AOT, SDS, Tween60, and Span80..... | 45 |
| Figure 5.2 | Water in oil emulsion stabilized by SDS. | 47 |
| Figure 5.3 | Polymerization result of SDS stabilized emulsion..... | 47 |
| Figure 5.4 | Polymerization result of AOT stabilized emulsion..... | 48 |
| Figure 5.5 | Product of #10 SC sample..... | 48 |
| Figure 5.6 | SEM photo of #1 SC. | 49 |
| Figure 5.7 | SEM photo of #2 SC. | 49 |
| Figure 5.8 | SEM photo of #3 SC. | 50 |
| Figure 5.9 | SEM photo of #4 SC. | 50 |
| Figure 5.10 | SEM photo of #5 SC. | 51 |
| Figure 5.11 | SEM photo of #6 SC. | 51 |
| Figure 5.12 | SEM photo of #7 SC. | 52 |
| Figure 5.13 | SEM photo of #8 SC. | 52 |
| Figure 5.14 | SEM photo of #9 SC. | 53 |
| Figure 5.15 | Flat surface of nanoparticles aggregation. | 54 |

LIST OF TABLES

| | Page |
|--|------|
| Table 3.1 Phase inverse water weight with different surfactant ratio (Span80/ Tween60). | 24 |
| Table 4.1 Formulation of nanoparticles of different cationic degrees. | 29 |
| Table 5.1 HLB and CMC of different surfactants. | 46 |
| Table 5.2 Experiments design of nanoparticle synthesis. | 46 |

NOMENCLATURE

| Symbol | Description |
|-----------------|--------------------------------|
| η_{∞} | Infinite shear viscosity |
| η_{sp} | Specific viscosity |
| $[\eta]$ | Intrinsic viscosity |
| c | Concentration |
| K_H | Constant of Huggins' Equation |
| K_K | Constant of Kraemer's Equation |
| pK_a | Acid dissociation constant |

1 INTRODUCTION

Application of nanotechnology in the oil and gas industry is just emerging. Recent research projects have shown that nanotechnology has the potential to solve or manage several problems in the petroleum industry. One of the speculated areas of application is in Enhanced Oil Recovery (EOR). EOR is especially important now because of the recent global rise in energy demand which is expected to be met by the oil and gas industry. The ability of nanoparticles to alter certain factors in the formation and in oil properties can be taken advantage of to enhance recovery (Ogolo 2012). This involves introducing these nanoparticles into formations and studying its effect on oil recovery.

Nanotechnology has been making its presence felt in the industry for some time, and many applications are already standard in petroleum refining. For instance, nanostructured zeolites are now used to extract up to 40% more gasoline than the catalysts they replaced (Ratner 2002, Crane 2002). The most obvious application of nanotechnology for upstream operations is development of better materials (Jackson 2005, Mokhatab 2006). The oil industry needs strong, stable materials in virtually all of its processes. By building up such substances on a nanoscale, it could produce equipment that is lighter, more resistant and stronger. Nanotechnology could also help develop new metering techniques with tiny sensors to provide improved information about the reservoir. Other emerging applications of nanotechnology in oil reservoir engineering are in the sector of developing new types of “smart fluids” for Enhanced Oil Recovery, drilling, etc. (Zitha 2005, Chaudhury 2003, Wasan 2003) Among these are new nanoformulations of surfactants/polymers, microemulsions, colloidal dispersion gels

(CDG), biliquid foams (aphrons). More recent developments deal with so-called “nanofluids”. These are designed by introducing small volumetric fractions of nanosized solid particles to a liquid phase in order to enhance or improve some of the fluid properties. Nanofluids can be designed to be compatible with reservoir fluids/rocks and be environment friendly. Some newly developed nanofluids have shown extremely improved properties in such applications as drag reduction, binders for sand consolidation, gels, products for wettability alternation, and anticorrosive coatings (Chaudhury 2003, Wasan 2003).

However, almost all the nanoparticles used in reservoir engineering are not water-absorbing particles, such as silica (Oleksandr 2015, Fawaz 2013), polysilicon (Kanj 2009, Dong 2006), carbon (Jie 2010) and magnetic nanoparticle (Saebom 2014), etc. These kinds of nanoparticles are non-deformable compared with gel nanoparticles (nanogels). Nanogels combine the properties of both hydrogels and nanomaterials: they show high water content, tunable chemical and physical structures, and good mechanical properties. And nanogels with novel properties and functions can be obtained by hybrid and/or graft, which is much easier than the polysilicon and alloy nanoparticles.

Hybrid nanogels can be classified based on their different properties into four kinds: a) core-shell nanogels; b) interpenetrated nanogels; c) embedded nanogels; d) porous nanogels. Core-shell nanogels can derive their multi properties by core-shell structure. Usually, the shell composition is different from core, such as different charges, different crosslink degree, and different polarity, etc. By two or more network interpenetrated with each other, interpenetrated nanogels are stiffer compared with traditional nanogels. Silica particles, magnetic powders are embedded into nanogels. The

embedded nanogels can have magnetic properties or some mechanical properties after embedding. Also, silica embedded nanogels are widely used to prepare porous nanogels.

Therefore, the purpose of this research is to develop novel nanogels that can be used for reservoir engineering.

First, review the mainly methods used to synthesize small gel particles, both the mechanism and kinetic of polymerization (emulsion and suspension). Second, synthesize nanogels that have salt and acid resistant properties. Third, synthesize a series of nanogels and find out the factors that influence particle size and morphology.

2 LITERATURE REVIEW

2.1 GENERAL FEATURES OF EMULSION & SUSPENSION POLYMERIZATION PROCESS

Both emulsion and suspension polymerization are heterogeneous polymerizations. There are usually two-phase systems in which starting monomer(s) and/or the resulting particles are in the form of a fine dispersion in an immiscible liquid. The polymerization initiator can be soluble in the monomer phase or the immiscible phase, or even not present during the particle formation. Emulsifier(s) or stabilizer(s) are used in addition to monomer(s) and immiscible liquid during the polymerization process to stabilize the monomer droplets and resulting particles. Particle within relatively narrow size ranges from 50nm to 1-2mm or larger can be obtained from emulsion and/or suspension polymerization.

2.1.1 Compositions of Polymerization. The choice of monomer in a microgel/nanogel preparation is vital in determining the resultant particle's properties. The monomer determines the swelling ratio of the particles. Additional properties, such as conductivity and functional groups which govern how the particle will respond to changes in the environment, can also be added into particles by monomer determination. One of the major advantages of microgel/nanogel is the ease at which the properties can be altered using the monomers and co-monomers.

The crosslinker in the particle is important, as the crosslink density controls the swelling ratio and mechanical strength of the particles. Also, crosslinker is the key point to make gel particles instead of polymer particles.

The initiator used in the particle preparation can affect the mechanism and properties of the particles. It can affect the type of polymerization, the yield, and the particle size. Additionally, the functionality of the initiator often influences the surface properties and charges on the particles which play a large role in determining how well the particles can be redispersed in solvent.

There are two kinds of polymerization system: oil in water and water in oil. For the continuous phase, it can affect the particle size, size distribution, and yield, etc. Viscosity and solubility are the two things mainly concerned.

Except oil in water and water in oil polymerize system, a new system (water or oil in supercritical carbon dioxide (scCO₂)) has been used as polymerize system. Compared with other polymerization medium, CO₂ is inexpensive, non-toxic, non-flammable, and readily available in high purity from a variety of sources. In addition, the separation of solvent from product is simplified because CO₂ reverts to the gaseous state upon depressurization, thus eliminating energy intensive drying steps. From a chemical perspective, CO₂ is relatively inert. However, solubility of most polymers in CO₂ is extremely low while the solubility of CO₂ in many polymers is substantial.

2.1.2 Mechanism of Polymerization. Emulsion and suspension polymerization are clearly distinguished by the following criteria.

- a) Initial state of the polymerization mixture;
- b) Kinetic of polymerization;

Emulsion polymerization:

For emulsion polymerization, dispersed phase (monomer phase) is immiscible with the continuous phase. Inverse emulsion polymerization is used to name polymerization occurring in water in oil (w/o) emulsion. Initiator is soluble in the

continuous phase. The decomposition process of initiator happens in continuous phase. Also, polymerization can be initiated by ultrasonic, radiation, etc.

Harkins (1945, 1947) has discussed the locus of the emulsion polymerization reaction and the function of the various phase present. During emulsion polymerization there are four phases which play an integral role in the over-all process. The water phase normally contains the “catalyst” or more properly, chain initiator; it is probable that the initial formation of free radicals takes place here. Dispersed in the water phase are emulsifier droplets of monomer; as long as these remain present, they serve to keep the other phases supplied with monomer. In the early stages of the reaction, soap micelles containing dissolved monomer are present; these serve as “generators” of polymer particles and they continue to serve this function until all the soap becomes adsorbed on the polymer-water interface produced by the polymerization. After polymerization has started, the fourth phase present consists of very small polymer particles which are swollen with monomer and these serve as the principal loci of polymerization.

Based on Harkin’s theory, Wendell (1948) has derived the kinetics of emulsion polymerization by separate the polymerization process into twofold. The first part is about the rate of polymerization in a single swollen polymer particle: rate of formation of free radicals, rate of escape of free radicals from reaction loci, rates of termination of free radicals in reaction loci and water solution, rate of polymerization of a free radical in a reaction locus, size, and number of reaction loci (polymer particle). And second part presents the factors determining the number of reaction loci produced in emulsion polymerization.

In Wendell's work, the free radicals are supposed only initiated in the external medium, and the rate of entrance of free radicals into a single locus is

$$\frac{dn}{dt} = \frac{\rho'}{N} \quad (1)$$

where ρ' is the over-all rate of entrance into all the N loci. And the rate of activity group transfer out of a locus is

$$\frac{dn}{dt} = -k_0 \alpha \frac{n}{v} \quad (2)$$

where k_0 is a specific rate constant for the event, n/v is the concentration of free radicals in a locus, and α is the interface area through which the transfer takes place. Destruction of free radicals is supposed to take place only by mutual termination so that the rate of destruction in a given locus is

$$\frac{dn}{dt} = -2k_t n \frac{n-1}{v} \quad (3)$$

where the factor of 2 arises from the fact that two free radicals are destroyed for each event of termination, k_t is the mutual termination specific reaction rate constant, and $(n-1)/v$ is the concentration of free radicals with which any of the n free radicals in a locus can react.

Then, three cases are highlighted. First, number of free radicals per polymer particle is small compared with unity; second, number of free radicals per polymer particle is approximately half of unity; third, number of free radicals per polymer particle is large compared with unity.

For the number of polymer particles, soap dissolved in the water (emulsifier dissolved in outer phase) is neglected. Thus, if S is the total amount of soap associated with one milliliter of water phase, it will consist of S_m grams in micellar form and S_p grams absorbed on polymer particles so that

$$S = S_m + S_p \quad (4)$$

If A , A_m , and A_p are the total interfacial area, area of micelles, and area of polymer particles, respectively,

$$\frac{A}{S} = \frac{A_m}{A_m} = \frac{A_p}{A_p} = \alpha_s \quad (5)$$

If ρ is the rate of formation of free radicals per milliliter of water solution, the rate of formation of new particles, dN/dt , is assumed equal to ρ and constant as long as micelles are present, so

$$\rho = \frac{dN}{dt} \quad (6)$$

If the ratio of monomer to polymer in the particle remains constant during the period in which new particles are being formed, the rate of increase in volume of a particle will be a constant which may be called μ , so if v is the volume of a particle

$$\frac{dv}{dt} = \mu \quad (7)$$

Thus the volume, $v_{\tau,t}$, at time t of a particle formed at time τ is

$$v_{\tau,t} = \mu(t - \tau) \quad (8)$$

Assuming a spherical particle, the area, $\alpha_{\tau,t}$, of this particle at time t is

$$\alpha_{\tau,t} = [(4\pi)^{\frac{1}{2}} 3\mu(t - \tau)]^{\frac{2}{3}} \quad (9)$$

By integration, at time $t=t_1$, when the soap micelles disappear, $A_p = \alpha_s S$, the total number of particles is

$$N = \rho t_1 = \rho^{\frac{2}{5}} \left(\frac{5\alpha_s S}{3\theta} \right)^{\frac{3}{5}} = 0.53 \left(\frac{\rho}{\mu} \right)^{2/5} (\alpha_s S)^{3/5} \quad (10)$$

The other idealized situation is that in which a given interfacial area always has the same effectiveness in collecting free radicals regardless of the size of the particle on which it is situated. This will give too few particles since a given interfacial area on the

very small micelles will be more effective than the same area on the larger polymer particles. At this situation

$$N = 0.370 \left(\frac{\rho}{\mu}\right)^{2/5} (\alpha_s S)^{3/5} \quad (11)$$

The actual situation should lie between these two situations. Thus

$$N = k \left(\frac{\rho}{\mu}\right)^{2/5} (\alpha_s S)^{3/5} \quad (12)$$

where $0.37 < k < 0.53$.

Suspension polymerization:

In suspension polymerization, monomer phase is immiscible with the continuous phase. Dispersed monomer phase is usually stabilized by stirring and/or emulsifier. Similar to emulsion polymerization, water in oil suspension polymerization also called inverse suspension polymerization. Initiator decomposes in the monomer phase.

Basis on the studies of Yuan (1991), polymerization kinetics in suspension polymerization are similar to those of bulk or solution polymerization, depending on the absence or present of a monomer diluents in the monomer phase. In this case, suspension polymerization is regarded as “microbulk” or “microsolution” polymerization, because the monomer droplets dispersed in continuous phase represent polymerization reactor/capsule.

2.2 SUSPENSION POLYMERIZATION

2.2.1 Process Description. In suspension polymerization, the initiator is soluble in the monomer, and monomer is insoluble in the polymerization medium. The volume ratio of the monomer phase to the polymerization medium is usually kept within 10-50%, but, in principle, it can be as high as unity. The monomer phase is, by means of a stirrer and a suitable droplet stabilizer, suspended in the medium in the form of small droplets

(microspheres). Under a certain temperature condition, the “monomer capsules” are converted directly to the corresponding polymer/gel particles of approximately the same size.

Examples of polymers/gels produced by oil in water (o/w) polymerization include polystyrene, poly(vinyl chloride), polyacrylates, and poly(vinyl acetate). Styrene-based resins and polymer supports are also obtained by o/w suspension co-polymerization of styrene and divinylbenzene. For all of these preparations the initiator is usually an azo compound (e.g. azo-bis-2-methylpropionitrile, AIBN), or an organic peroxide (e.g. benzoyl peroxide), and the polymerization is performed at a temperature of about 50-100°C. The typical droplet stabilizers used for o/w suspension polymerization are polyvinylpyrrolidone (PVP) and poly[(vinyl alcohol)-co-(vinyl acetate)]. The latter polymer is obtained by partial (85-92%) hydrolysis of poly(vinyl acetate). A wide range of other water soluble organic polymers including natural gums, cellulose ethers, and synthetic polymers are also used. Scarcely soluble inorganic salts such as talc, phosphates, and sulfates may also be employed, either alone or in combination with organic stabilizer.

Major examples of polymers produced by w/o suspension polymerization include polyacrylamide and water soluble acrylates. Acrylamide based polymer supports are also prepared by w/o suspension co-polymerization of acrylamide with bisacrylamide. Here, an aqueous solution containing the monomer(s) and the initiator is suspended in liquid paraffin or a chlorocarbon (polymerization medium), followed by polymerization at a temperature of 20-50°C. A water-soluble catalyst for w/o suspension polymerization is the combination of potassium peroxydisulfate and N,N,N',N'-tetramethylethylenediamine. Stabilizers used for w/o suspension polymerization include

ethylcellulose, cellulose acetate butyrate, and various amphiphilic oligomers such as Span and Tween.

For scCO₂ suspension polymerization, the monomer has very low solubility in the continuous phase. Most common monomers studied so far have been found to be quite soluble in CO₂ at moderate temperatures and pressures, and therefore few examples exist of CO₂-based emulsion or suspension polymerizations. Beckman (1989, 1994) has investigated the w/o emulsion polymerization of acrylamide in scCO₂ (AIBN, 65°C, 352bar, 1h). An amide functionalized perfluoropolyether surfactant was used to promote latex stabilization. The latex was observed to be more stable in the presence of surfactant, although high monomer conversions and molecular weights were also obtained without the stabilizer. Since water and CO₂ have very low miscibility, the development of other inverse suspension polymerization techniques is likely to be a profitable area of research, particularly given the recent advances in the synthesis of surfactants for the formation of water in CO₂ microemulsions. In principle, the use of CO₂ as a medium for the oil in oil suspension polymerization of lipophilic monomers might also be a possibility, providing that the monomers exhibit sufficient miscibility gaps at reasonable CO₂ densities. For example, Beckman (1994) has carried out the co-polymerization of cyclohexene oxide in scCO₂ under conditions where a CO₂-rich layer and a monomer-rich layer were observed from the outset, although no attempt was made to emulsify the two phases. Other studies have shown that perfluorocarbon liquids are quite versatile solvents for the suspension polymerization of a range of lipophilic and hydrophilic monomers, but the high cost of these solvents is a major drawback. By changing monomer soluble initiator to CO₂ soluble initiator, emulsion polymerization can also be done.

Quality of the polymer particle products obtained by suspension polymerization depends, in addition to reactor design, on operational parameters governing the overall stability of the suspension system. In practice, efficient management of a suspension polymerization process is as much an art as it is based on exact scientific principles. Figure 2.21 shows examples of polymer particles produced by suspension polymerization. In micrograph A, the particles are irregular agglomerates of smaller microspheres. This product was obtained from a low viscosity monomer mixture and a poorly stabilized suspension system. Micrograph B, on the other hand, shows relatively uniform individual microspheres obtained from a normal polymerization run under carefully controlled conditions (Arshady 1974).

2.2.2 Size Control & Morphology. Suspension polymerization can, in principle, be employed to produce polymer particles within any size range, from about 100nm up to about 1-2mm or even larger. For the routine practice of addition polymerization of vinyl monomers, however, suspension polymerization is suitable for polymer particles within the size range of about 20 μ m to 2mm.

The average size of the monomer droplets can be readily controlled by varying the stirring speed, volume ratio of the monomer to suspension medium, concentration of the stabilizer, and the viscosities of both phases according to the following equation. This equation represents most of the empirical relationships reported by Arshady and Ledwith (1983), Hopff and coworkers (1965), Kavarov and Babanov (1959), Mersmann and Grossman (1980), and Sculles (1976):

$$\bar{d} \equiv k \frac{D_v R v_D \epsilon}{D_s N v_m C_s} \quad (13)$$

where \bar{d} is average particle size; k is parameters such as apparatus design, type of stirrer, self-stabilization, etc.; D_v is diameter of vessel; D_s is diameter of stirrer; R is volume ratio of the droplet phase to suspension medium; N is stirring speed; ν_d is viscosity of droplet phase; ν_m is viscosity of the suspension medium; ϵ is interfacial tension between the two immiscible phases; and C_s is stabilizer concentration.

An important aspect of polymer particles obtained by suspension polymerization is the surface and bulk morphology of the product. This morphology is basically related to the degree by which the polymer dissolves swells or precipitates in the monomer phase. When the polymer is soluble (or swellable) in its monomer mixture, the resulting particles have a smooth surface and a relatively homogeneous (nonporous) texture. On the other hand, when the polymer is not soluble (or swellable) in its monomer mixture, the final particles have a rough surface and a porous morphology.

2.3 EMULSION POLYMERIZATION

2.3.1 Process Description. Emulsion polymerization can be performed in the presence of added surfactant (conventional emulsion polymerization) or in the absence of added surfactant (surfactant-free emulsion polymerization). In the surfactant-free emulsion polymerization method, the continuous phase must have a high dielectric constant (e.g. water) and ionic initiators are employed (e.g. $K_2S_2O_8$). The charged polymer chains formed during polymerization act as surfactant molecules and stabilize the growing particles.

2.3.2 Conventional Emulsion Polymerization. In emulsion polymerization, the monomer is insoluble (or scarcely soluble) in the polymerization medium, but it is

emulsified it by the aid of a surfactant (emulsifier or soap). The initiator is, unlike in suspension polymerization, soluble in the medium, and not in the monomer. Under these

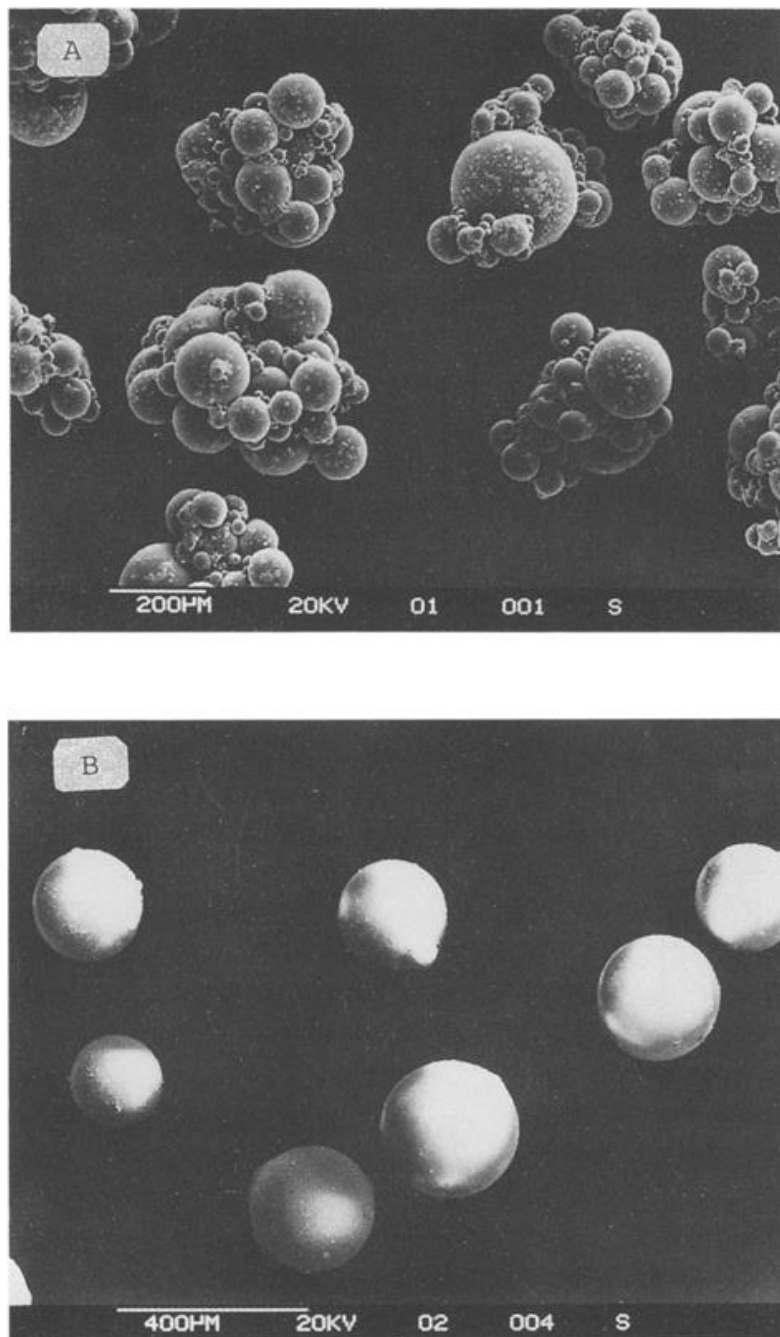


Figure 2.1. SEM photo of polymer samples produced by suspension polymerization.

conditions, the monomer is present in the mixture partly in the form of droplets (about 1-10 μ m or larger), and partly in the form of soap-coated micelles (ca. 50-100 \AA), depending on the nature and concentration of the emulsifier. A small percentage of the monomer is also molecularly dissolved in the medium. For example, solubility of styrene in water at 70°C is about 4g/L.

For o/w emulsion polymerization (e.g. styrene in water), potassium peroxydisulfate and sodium dodecylsulfonate are commonly used as initiator and emulsifier, respectively. Combinations of ionic and nonionic emulsifiers may also be used. An interesting example is the use of sodium dodecylsulfonate and Triton X-100, as reported by Woods et al. (1968) for the preparation of monodisperse polystyrene particles.

For water soluble monomers, an aqueous solution of the monomer is emulsified in a water immiscible liquid, in the presence of a w/o emulsifier, and an oil soluble initiator. Examples of w/o emulsion polymerization are those of acrylamide and sodium 4-vinylbenzenesulfonate in toluene, in the presence of benzoyl peroxide initiator. Fatty esters of polyhydroxy compounds (e.g. sorbitan monooleate) are often used as w/o emulsifiers.

2.3.3 Soap-free Emulsion Polymerization. Figure 2.2 shows the salient features of surfactant-free emulsion polymerization. Thermal decomposition of the ionic initiator ($S_2O_8^{2-}$) initiates free-radical polymerization. The oligomers produced are surface active and form nuclei when the length of the oligomers exceeds the solubility limit of the solvent. The nuclei then undergo limited aggregation, thereby increasing the surface charge until electrostatic stabilization is achieved. Further particle growth occurs through

absorption of monomer and/or oligomeric chains. This process results in a decrease in the concentration of oligomers to below the critical value required for particle formation. Polymerization continues within the particles until another radical species enters the growing particle and termination occurs. The key feature of surfactant-free emulsion polymerization is that the particle nucleation period is very short which ensures a narrow

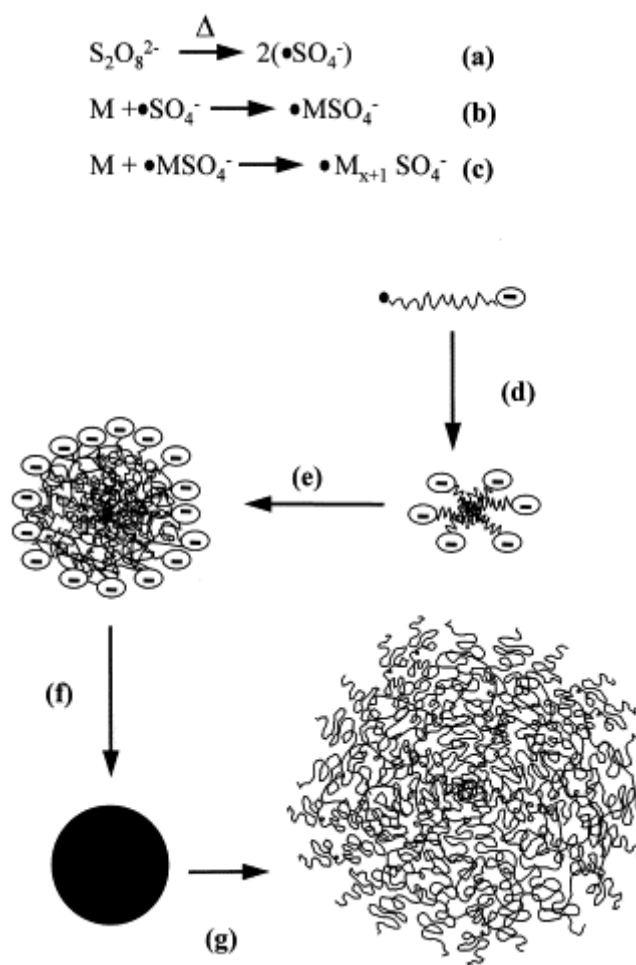


Figure 2.2. Mechanism for the preparation of microgel particles by surfactant-free emulsion polymerization. The steps shown are initiator decomposition (a), initiation (b), propagation (c), particle nucleation (d), particle aggregation (e), particle growth (in a poor solvent) (f), and particle swelling in a good solvent (g).

particle size distribution. The final particle size achieved by surfactant-free emulsion polymerization increases with electrolyte concentration and decreasing initiator concentration.

Monodisperse poly(NIPAM) particles may be formed during surfactant-free emulsion polymerization in the absence of added crosslinking monomer. Thus, NIPAM appears to act as its own crosslinking monomer; however, the efficiency of crosslinking is clearly improved when crosslinking monomer are employed.

An alternative method used for the preparation of microgel system involves polymerization using a good solvent. Staudinger and Husemann (1935) polymerized dilute DVB solutions and obtained soluble products with low intrinsic viscosity. Antionetti and Rosenauer (1991) re-investigated the DVB system and reported broad particle size distributions. Okay and Funke (1990) used an analogous anionic polymerization method whereby 4-tert-butylstyrene was copolymerized with DVB in heptanes to yield microgel particles. The size distributions for these products were also broad.

The above examples reveal that particle formation using good solvents for the polymer suffers from poor particle size uniformity. The primary reason for this is a lack of electrostatic stabilization during polymerization; pendant vinyl groups are able to react with radical sites on neighboring polymer chains. Network growth may therefore occur by reaction with neighboring particles at any time during the polymerization, resulting in broad particle size distributions. However, it is likely that particles formed using this method have a relatively uniform distribution of co-monomers because precipitation of high molecular weight chains does not occur.

2.3.4 Size Control & Morphology. The size of latex particles in emulsion polymerization has no direct relationship with the size of the initially formed monomer droplets or micelles. These do not contain any initiator and, hence, are not directly converted to the corresponding polymer particles. Instead, the fraction of the monomer molecularly dissolved in the polymerization medium plays a key role in determining the size of the final particles. The size of the latex particles in emulsion polymerization is also influenced by a number of other factors, including emulsifier concentration and polymerization temperature.

The size of the particles decreases as the temperature of polymerization increases. This observation is in accordance with the nucleation mechanism, and reflects the dependence of particle size on the rate of nucleation (\equiv rate of polymerization). Other kinetic parameters which control the rate of polymerization reaction, such as concentrations of initiator, emulsifier, and salt, also influence the size of the latex particles. Salt concentration controls the viscosity and ionic strength of the medium, both of which influence the course of the nucleation process.

2.4 OTHER TECHNIQUES

Dispersion polymerization is also a widely used method to get particle gels. Monomer is soluble in polymerization medium. The resulting polymer/gel is insoluble in the dispersion medium and therefore phase separation occurs at an early stage in the reaction. Here, only dispersion polymerization in CO₂ is reviewed.

In the presence of 2-4% w/v of a CO₂-soluble polymer PFOA, the phase behavior was different from in the absence of stabilizer one for precipitation polymerization of MMA. As the reaction proceeded (65°C, 204bar, initiated by AIBN), a stable, opaque-

white colloidal dispersion was formed in the reaction vessel. When examined by scanning electron microscope, the product was found to consist of uniform spherical particles, with average diameters in the range 1.2-2.5 μm . The CO_2 -philic nature of fluoroalkyl substituents on the stabilized caused extension of the PFOA chain trajectory into the continuous phase, thus giving rise to steric stabilization and preventing particle flocculation.

Vinyl acetate and styrene had also been polymerized via dispersion polymerization on the use of PFOA as a stabilizer. The particle morphology of polystyrene synthesized by dispersion polymerization in scCO_2 is shown in Figure 2.3.

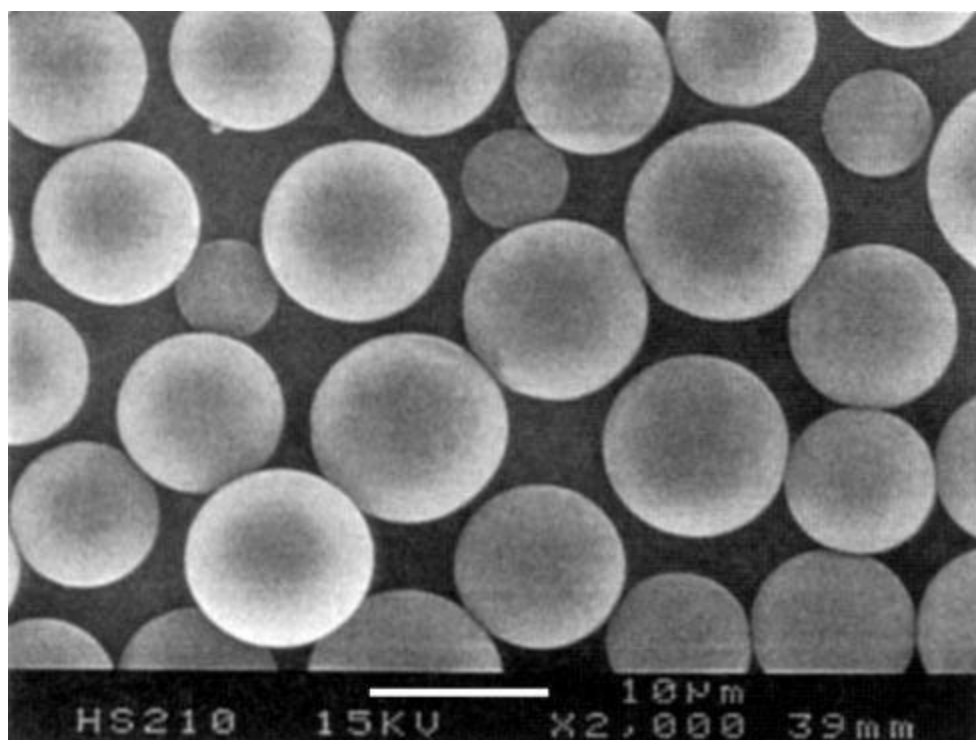


Figure 2.3. SEM photo of polystyrene particles synthesized in scCO_2 by dispersion polymerization.

Random copolymers of FOA and styrene were synthesized as stabilizers for the dispersion polymerization of 2,6-dimethylphenol in scCO₂ by oxidative coupling polymerization, although these polymers were not as effective as diblock copolymer stabilizers.

Helium presents in CO₂ could have significant effects on the average particle size and particle size distributions of PMMA samples synthesized in scCO₂ using PFOA as the stabilizer. Solvatochromatic studies suggested that this was due to a decrease in the solvent strength of the continuous phase.

Silicone polymers are attractive as stabilizers, because they are soluble in CO₂ and considerably less expensive than their fluorinated counterparts. In 1996, a commercially available methacrylate-terminated poly(dimethylsiloxane) (PDMS) macromonomer was used for the dispersion polymerization of MMA in CO₂. These polymerizations were carried out in scCO₂ using AIBN initiator.

Howdle and co-workers (1999, 2000) used PDMS macromonomer stabilizer for the dispersion polymerization of MMA in scCO₂.

Lepillien and Beckman (1997) synthesized a series of surfactants based on a poly(MMA-co-hydroxyethyl methacrylate) backbone with varying percentages of a CO₂-philic poly(perfluoropropylene oxide) graft. The stabilizers were effective for the free radical dispersion polymerization of MMA in scCO₂, and studies were made to find the optimum “anchor-to-soluble balance” (the most effective ratio between the CO₂-phobic backbone and the CO₂-philic solubilizing grafts).

Canelas et al. (1996) showed that PS-b-PFOA stabilizers are very effective for the free radical dispersion polymerization of styrene in scCO₂ (AIBN, 65°C, 345 bar, 24h),

and that the total molecular weight of stabilizer has a strong effect on the average particle size and particle size distribution of the resulting colloidal polystyrene. Stabilized concentrations of 2.5-15% based on the monomer were used, and the average particle size varied from 1.15 down to 0.31 μm , depending on the stabilizer concentration. The PS particle size was found to be influenced quite significantly by the density of the CO_2 continuous phase (pressure) and also the presence of helium.

Uniform PMMA particles could be synthesized in scCO_2 by dispersion polymerization using either PFOA stabilizer or a commercially available graft copolymer surfactant (PDMS-g-pyrroldonecarboxylic acid). When mixtures of both stabilizers were used, smaller, more regular PMMA particles were formed.

3 PREPARATION OF MICROEMULSION

3.1 MATERIALS

Acrylamide, 98+% (AM) and N-decane, 99% were from Alfa Aesar. N,N'-methylene bisacrylamide, 99% (MBAA), and Polyethylene glycol sorbitan monostearate, (Tween 60) were purchased from Sigma-Aldrich. [2-(acryloyloxy) ethyl] trimethylammonium chloride solution, (AETAC) was from Aldrich. Sorbitan monooleate, (Span 80) viscosity 1200-2000 mPa•s (20 °C) was from Fluka. Mineral oil (light), was from Fisher Chemical. Water used in the following experiments was deionized (DI) water and all the chemicals were used as received.

3.2 SURFACTANT RATIO SELECTION

In order to get microemulsion for the polymerization of nanoparticles, different constituents were studied. Because the nanoparticles synthesized were mostly hydrogel, which was polymerized by hydrophilic monomer and crosslinker, via suspension polymerization. The emulsion type should be water in oil (w/o).

During the polymerization process, a large amount of heat can be exposed by polymer chain growth and termination. The heat provided can cause an autoaccelerate effect, which also named as Trommsdorff effect, to reduce the stability of polymerization system. As a result, heterogeneous particles or even bulk gel can be synthesized via the polymerization instead of homogeneous nanoparticles.

In order to enhance the heat transmit, oil phase should have low viscosity and density, but also a relatively high boiling point. Branched and/or light alkane, such as n-

octane, n-nonane, n-decane, and iso-tetradecane, etc., were good choices to form the microemulsions. Boiling points of different n-alkane were shown in Figure 3.1.

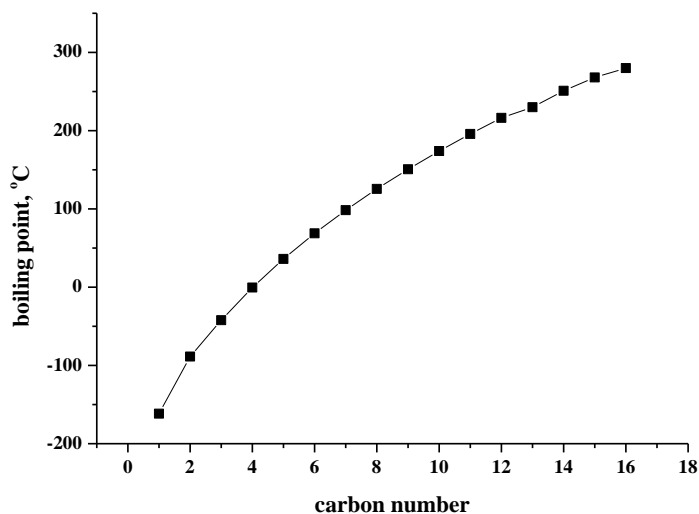


Figure 3.1. Boiling points of different n-alkane (from C₁ to C₁₆)

Emulsifier is the most important component in microemulsion. Usually, the concentration of emulsifier in microemulsion is much larger than (ten times and more) emulsion. The solubilization of aqueous solution in microemulsions is strikingly influenced by the chemical structure of oil and surfactant mixture. There exists a preferred oil chain length for a specific surfactant which solubilizes more water than others. When using nonionic surfactants mixture as emulsifier to formulate microemulsion, the solubilization of water is a function of surfactants ratio. There exist a certain value of surfactants ratio for water solubility reaches its peak.

Tween60 and Span80 were the two surfactants used to forming w/o microemulsion. The hydrophilic-lipophilic value of Tween60 is 14.9 and Span80 is 4.3.

By mixed different ratio of Span80 and Tween60 together, different HLB value of surfactant mixture can be got. The calculation of mixture HLB was shown in the following equation.

$$HLB_{AB} = \frac{HLB_A * W_A + HLB_B * W_B}{W_A + W_B} \quad (14)$$

where HLB_A is the HLB value of surfactant A, HLB_B is the HLB value of surfactant B, HLB_{AB} is the HLB value of surfactant mixture of A and B, W_A and W_B are the surfactant weight of A and B separately.

Surfactant mixtures of different surfactants ratio (Span80/ Tween60) were prepared by mix different amount of Span80 and Tween60 together. Then, n-decane was mixed with the surfactant mixtures. Water was added dropwise and the weight of water was shown in Table 4.1 when emulsion type turned from water in oil to oil in water (phase inverse) or emulsion became unstable (phase separate in 5 minutes).

Table 3.1. Phase inverse water weight with different surfactant ratio (Span80/ Tween60).

| | | | | | | | | | |
|------------------|-------|-------|-------|-------|------|------|------|------|------|
| Surfactant ratio | 1:9 | 2:8 | 3:7 | 4:6 | 5:5 | 6:4 | 7:3 | 8:2 | 9:1 |
| HLB value | 13.84 | 12.78 | 11.72 | 11.52 | 9.6 | 8.54 | 7.48 | 6.42 | 5.36 |
| Water weight/ g | 0.69 | 0.75 | 3.34 | 3.33 | 5.09 | 5.95 | 9.61 | 7.00 | 5.09 |

When Span80 to Tween60 ratio is 7:3, the surfactant mixture can solubilize 9.61g water before phase inverse. Compared with other ratios, 7:3 can solubilize largest amount of water and was chosen for the following experiments.

3.3 MICROEMULSION DETERMINATION

Electrical conductivity was used to determine phase behavior of oil-surfactant-water mixture. Electrical conductivity is a structure sensitive property and has been used to determine phase behavior of emulsions stabilized by nonionic surfactant. Drop test was also used to determine phase behavior. Compared to measuring electrical conductivity, drop test is a far more simply method. Toke one drop from the emulsion; drop it in to a test tube filled with water. If the drop of emulsion spread quickly and form a thin film on the water surface, the emulsion was regarded as oil in water emulsion; if the drop of emulsion staid as a sphere or ellipsoid droplet (usually on the water surface) unmixed with water, the emulsion was regarded as water in oil emulsion.

Electrical conductivities of emulsions were measured when the emulsion was not sticky. For example, the electrical conductivity versus water/oil ratio shown in Figure 3.2 while the electrical conductivity of aqueous solution (50wt.% acrylamide) is $30.4\mu\text{S}$. Aqueous solution was added to the mixture of surfactants and oil dropwise under 40°C . The emulsion was homogenized by magnetic stirring bar until aqueous solution was fully separated. Then, measuring rod was put into emulsion to measure electrical conductivity.

As shown in Figure 3.2, the electrical conductivity changed exponentially with the volume fraction of aqueous solution increasing. These changes are caused by the occurrence of a percolation transition. In the percolation model, conductivity remained low up to a certain volume friction of water.

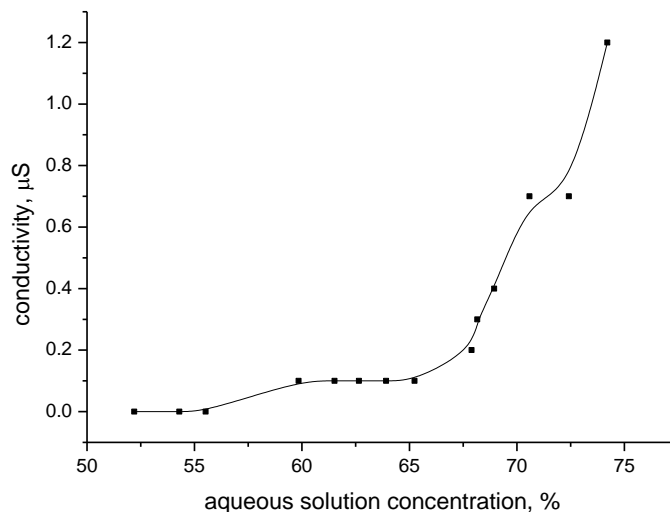


Figure 3.2. Variation of electrical conductivity of emulsion as a function of aqueous solution content.

These conducting aqueous droplets were isolated from each other in non-conducting continuous oil phase. Hence, these droplets contributed little to the conductivity when aqueous solution concentration below 65wt.%. However, as the weight fraction of aqueous solution increasing, some of these conductive droplets began to contact and formed clusters, which were sufficiently close to each other. For the weight fraction of aqueous solution further increased, more droplets formed clusters and even transferred to aqueous channels.

When the weight fraction of aqueous solution was 62 to 69wt.%, emulsion type turned from water in oil to oil in water. Also, at this water content range, emulsion turned from turbid to transparent.

3.4 PSEUDO-TERNARY PHASE DIAGRAM

Pseudo-ternary phase diagram was an intuitionistic way to determine the emulsion type. After figure out the boundary of emulsion and microemulsion, it was easy to distinguish microemulsion by amount of the compositions.

The test points were shown in Figure 3.3. The ratio of Surfactants mixture to Oil was kept same in each line. And the amount of aqueous solution was increased from 10 to 100wt.%. Actually, after emulsion type changing from w/o to o/w, aqueous solution was stopped adding.

The points, at which emulsion type changes, were used to plot pseudo-ternary phase diagram.

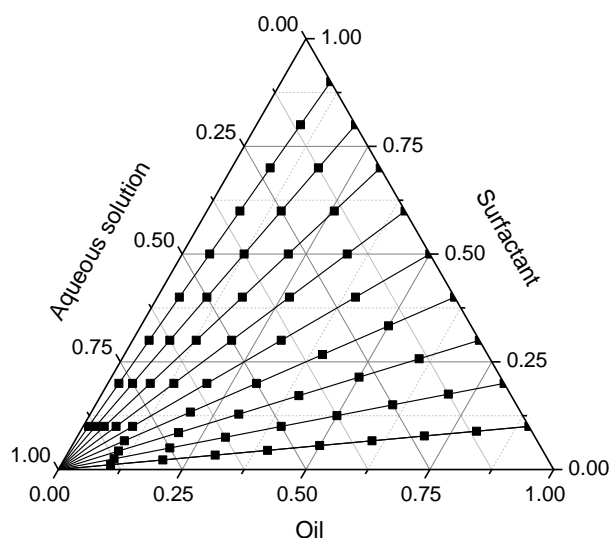


Figure 3.3. Experiment design for Pseudo-ternary phase diagram.

4 SYNTHESIS & EVALUATION OF CATIONIC NANOPARTICLES

4.1 MATERIALS

Acrylamide, 98+% (AM) and N-decane, 99% were from Alfa Aesar. N,N'-methylene bisacrylamide, 99% (MBAA), acetone, for HPLC $\geq 99\%$ and Polyethylene glycol sorbitan monostearate, (Tween 60) were purchased from Sigma-Aldrich. [2-(acryloyloxy) ethyl] trimethyl-ammonium chloride solution, (AETAC) was from Aldrich. Sorbitan monooleate, (Span 80) viscosity 1200-2000 mPa•s (20 °C) was from Fluka. . Ammonium persulfate, BP179-100 (APS) was from Fisher bioreagent. Sodium chloride, certified ACS crystalline was from Fisher Chemical. Hydrochloride acid, for analysis, ca. 37% solution in water was from Acros Organics. Water used in the following experiments was deionized (DI) water and all the chemicals were used as received.

4.2 SYNTHESIS OF CATIONIC NANOPARTICLES

A free-radical suspension polymerization method was used to prepare nanoparticles of poly[acrylamide-co-[2-(acryloyoxy) ethyl] trimethyl-ammonium chloride]. The crosslinker was MBAA. In a typical experiment, 42.54g AM, 0.2g MBAA, and 25.57g AETAC were dissolved in 31.69g water to prepare aqueous solution. 21g Span80 and 9g Tween60 were mixed under magnetic stirring at 40°C.

Then 50g aqueous solution, 30g surfactants mixture, and 20g of n-decane were adding to a 250mL three neck round bottom flask equipped with a reflex condenser and a stirrer. After nitrogen purging for 15 minutes, 0.2g 15wt.% ammonium persulfate solution was added to the system dropwise to act as a thermal initiator under 40°C. Stirring rate was increased from 300 to 500rpm at the same time. Polymerization process

was allowed to continue for 1.5 hours. The nanoparticles were precipitated from the microemulsion when dropped microemulsion into acetone. Then, 4000rpm ultracentrifuge was used to separate nanoparticles and acetone for 20 minutes before removing the supernatant. The acetone wash- ultracentrifuge procedure was repeated for three times in order to remove decane, surfactant and unreacted monomers. Afterwards, precipitates were collected and dried in vacuum oven for one day at a temperature corresponding to the acetone boiling point (60°C). Then these white powders were dissolved and used in the evaluation process. The formulation of nanoparticles of different cationic degrees was shown in Table 4.1.

Table 4.1. Formulation of nanoparticles of different cationic degrees.

| cationic degree/ % | 0 | 5 | 10 | 15 | 20 |
|------------------------|-------|-------|-------|-------|-------|
| AM/ g | 18.9 | 16.51 | 14.51 | 12.76 | 11.24 |
| AETAC/ g | 0 | 2.96 | 5.49 | 7.67 | 9.57 |
| MBAA/ g | 0.06 | 0.06 | 0.06 | 0.06 | 0.06 |
| water/ g | 11.04 | 10.46 | 9.95 | 9.51 | 9.13 |
| n-decane/ g | 40 | 40 | 40 | 40 | 40 |
| Surfactant mixture/ g | 30 | 30 | 30 | 30 | 30 |
| 15wt.% APS solution/ g | 0.2 | 0.2 | 0.2 | 0.2 | 0.2 |

4.3 EVALUATION OF CATIONIC NANOPARTICLES

4.3.1 Morphology of Cationic Nanoparticles. FEI Quanta 600 FEG Extended Vacuum Scanning Electron Microscopoe (ESEM) and FEI Helios 600 Scanning Electron Microscope (SEM) were used to characterize the morphology of cationic nanoparticles. For ESEM, cationic nanoparticles were dispersed in 1wt.% NaCl solution and completely

swelling before measurement. Nanoparticles were put in chamber and measured at -5°C and high vacuum degree ($1.38 \times 10^{-3}\text{Pa}$).

The morphology of swelled cationic nanoparticles was shown in Figure 4.1. A freeze-dry process were taken inside chamber (froze to 0°C and low vacuum degree, then, increased vacuum degree to $1.38 \times 10^{-3}\text{Pa}$). Nanoparticles were aggregated with each other and the edges were not clear. Nanoparticles were supposed soft after swollen, and stacked together with each other. When water was dragged out, the polymer network cannot support nanoparticles as sphere. Hence, nanoparticles in ESEM photo were not isolated and spherical.

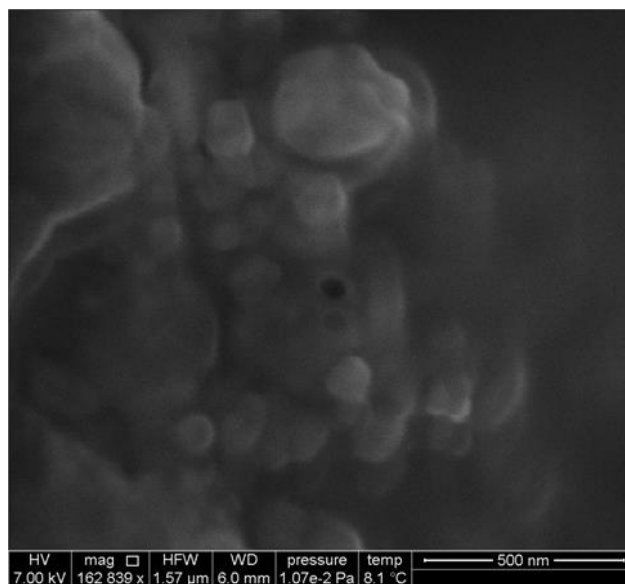


Figure 4.1. Morphology of cationic nanoparticles swelled in 1wt.% NaCl (ESEM).

SEM was also used to measure the morphology of cationic nanoparticles. Because SEM required sample to be dried, cationic nanoparticles powder was used. During the drying process, the surface of powder (at least 100 times compared to nanoparticle) was

changed due to the shrinkage of nanoparticles. Here, powders were cracked into several parts and nanoparticles could be found in the fractures of powders. Morphology of nanoparticles was shown in Figure 4.2 and Figure 4.3.

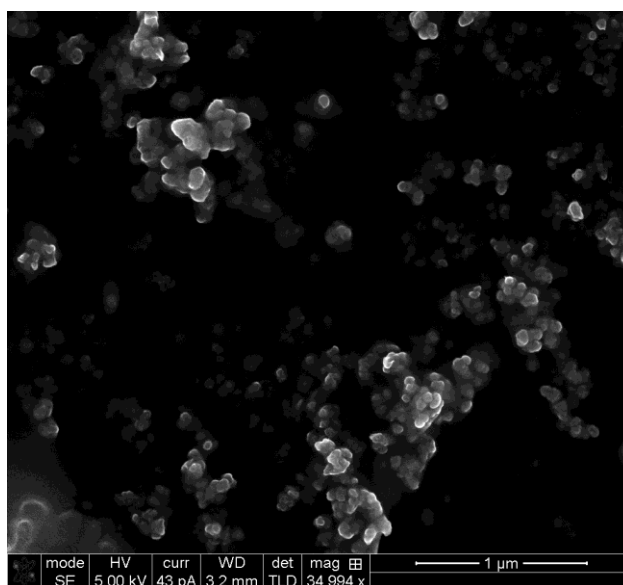


Figure 4.2. Morphology of cationic nanoparticles (SEM).

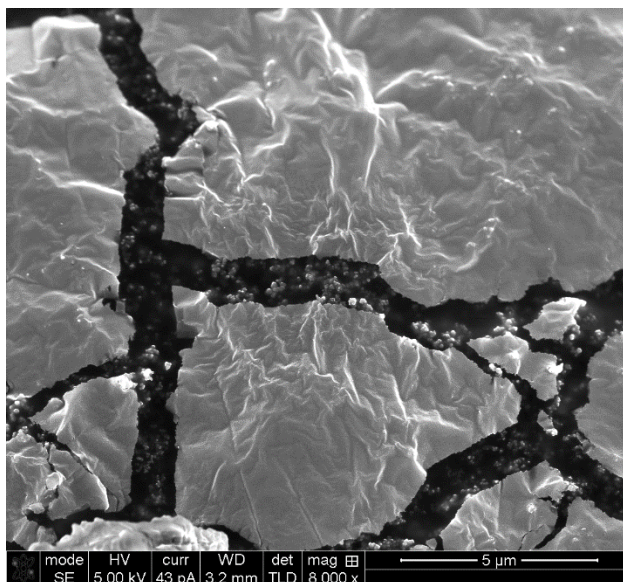


Figure 4.3. Nanoparticles in the fractures of a powder.

4.3.2 Effect of Cationic Degree of Nanoparticles. Nanoparticles of different cationic degree were dispersed in 1wt.% sodium chloride solution. Before measuring the particle size distribution, 0.45 μ m filter was used to remove aggregations of nanoparticles. The diameters of nanoparticles were shown in Figure 4.4.

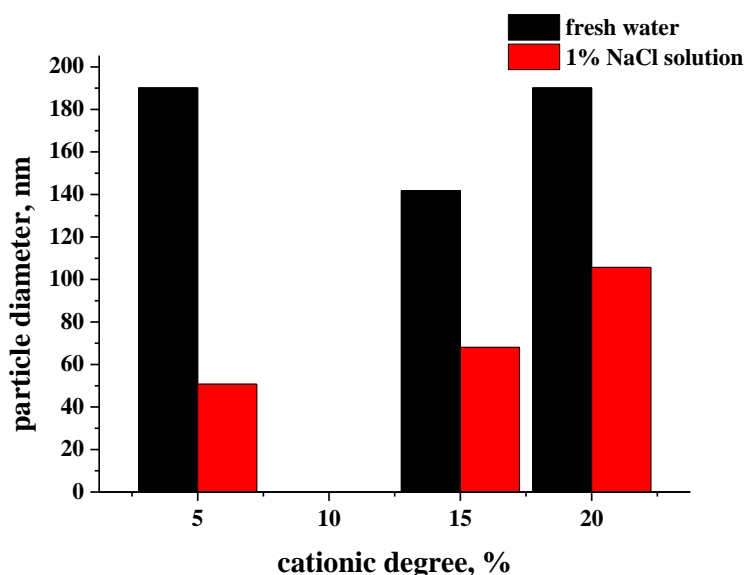


Figure 4.4. The average diameter of fully swelled nanoparticles in deionized water (black column) and 1wt.% NaCl solution (red column).

When dispersed in deionized water, nanoparticles of 5% and 20% cationic degree can swell to an average diameter of 190nm, while nanoparticles with 15% cationic degree can swell to 145nm. When the salinity of surrounding solution increased to 1%, all the nanoparticles were deswelled. However, different cationic degree provided different saline resistance. Nanoparticles of 5% cationic degree shrank to a diameter of 50nm, and nanoparticles of 15% and 20% cationic degrees shrank to diameters of 65nm and 110nm respectively.

As cationic degree increased, the nanoparticles became less sensitive to salinity water. For nanoparticles of 5% cationic degree, when the solution changed from deionized water to 1wt.% NaCl solution, particle diameter can shrank 3.8 times. In terms of volume change, the nanoparticles were shrank around 55 times. However, for nanoparticles of 20% cationic degree, the diameter only shrank less than 2 times and the volume change less than 6 times.

This might be influenced by the $-N(CH_3)_3^+$ groups on the polymer chain of cationic nanoparticles. For PAM nanoparticles, cations can reduce electrostatic repulsion between $-COO^-$ by screening effect. Thus, the swelling ratio of PAM nanoparticles will significantly decrease when the medium was changed from fresh water to salinity water, due to the osmotic pressure inside PAM nanoparticles decreased. However, when cationic monomers were introduced to nanoparticles, the screening effect induced by cations was weakened compared to pure PAM nanoparticles. Though the swelling ratio in fresh water decreased as cationic degree increased, it changed less when contacted with saline solution. The increased electrostatic repulsion between polymer chains made cationic nanoparticles in sensitive to salt.

For polymer solutions, viscosity can reflect the degree of chain entanglement. The viscosity of dispersion can be used to determine the electrical repulsion among nanoparticles. The stronger repulsion among nanoparticles, the higher viscosity dispersion was.

Cationic nanoparticles were dispersed into saline of different salt concentrations and their viscosities were measured at 25°C. Shear rate was chosen from 1.22 to 122s⁻¹.

Infinite shear viscosity was got from viscosity vs. shear rate plot by extended the curve.

The viscosity data of nanoparticle dispersions were shown from Figure 4.5 to Figure 4.8.

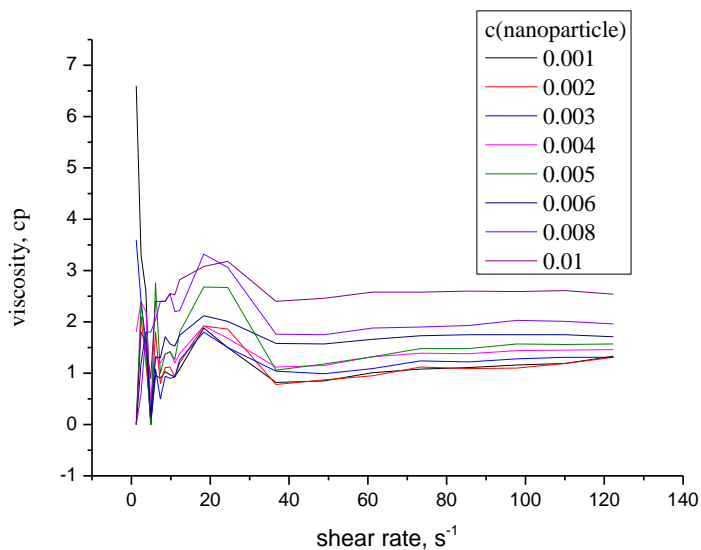


Figure 4.5. Dispersion viscosity of 0% cationic degree nanoparticles (concentration from 0.1 to 1wt.%).

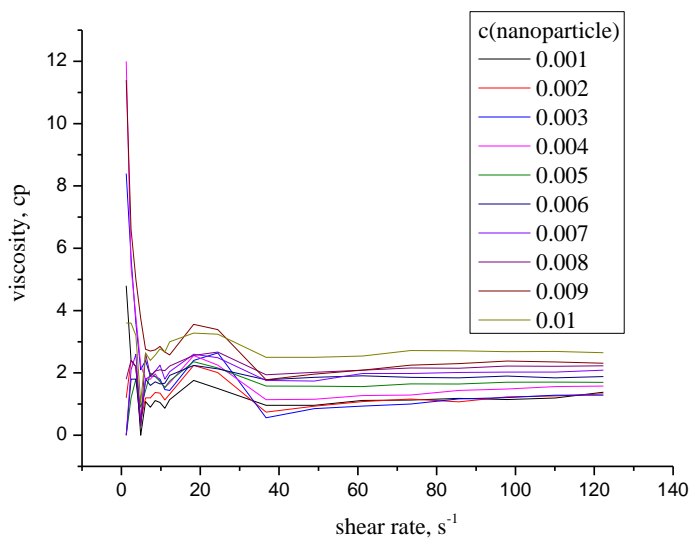


Figure 4.6. Dispersion viscosity of 5% cationic degree nanoparticles (concentration from 0.1 to 1wt.%).

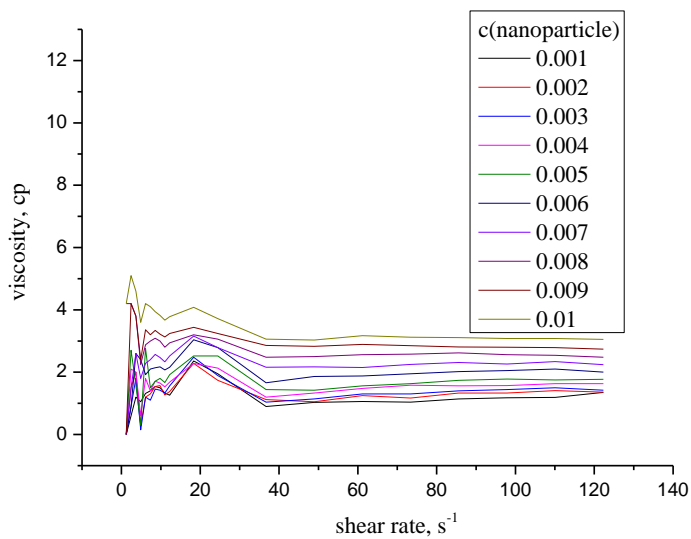


Figure 4.7. Dispersion viscosity of 10% cationic degree nanoparticles (concentration from 0.1 to 1wt.%).

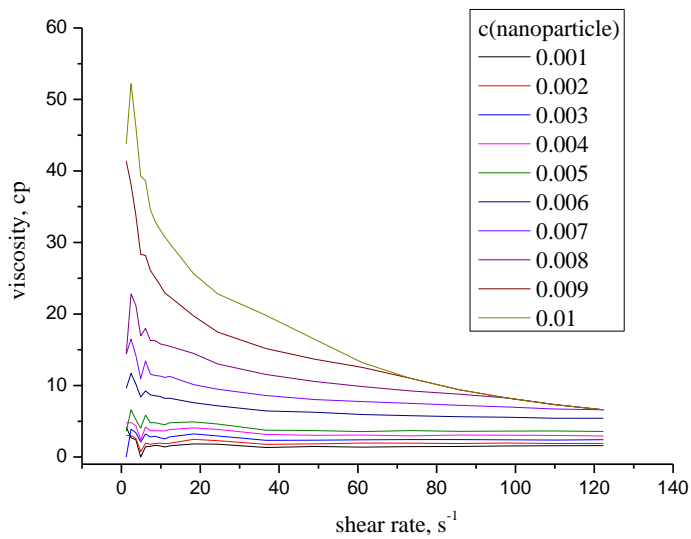


Figure 4.8. Dispersion viscosity of 15% cationic degree nanoparticles (concentration from 0.1 to 1wt.%).

After extending curves, infinite shear viscosity, η_{∞} can be got. Infinite shear viscosity against concentration plot was shown in Figure 4.9 at various cationic degrees.

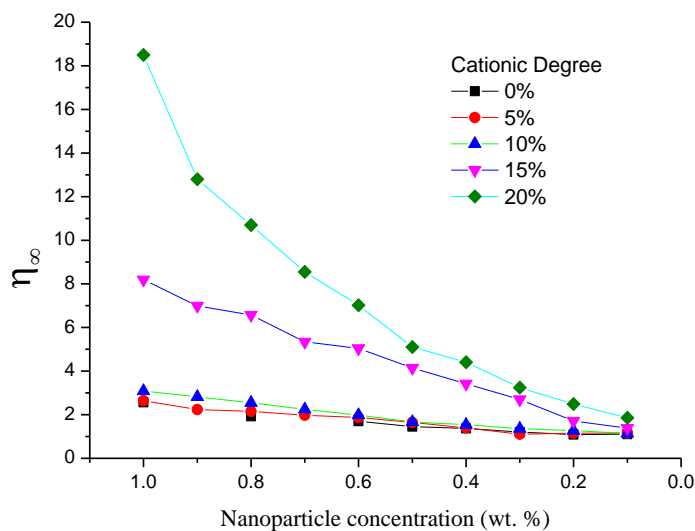


Figure 4.9. Infinite shear viscosity of cationic nanoparticles.

All the dispersion viscosities of nanoparticles decreased with the decreasing of nanoparticle's concentration. However, the critical point, at the slope of viscosity vs. concentration curve sudden change, was not obvious. Dispersion's viscosity was increased when cationic degree increased from 0 to 20% (though the viscosities were almost same from 0 to 10%).

Intrinsic viscosity had been used to determine the contribution of single molecule to system's viscosity, which means intrinsic viscosity can reflect repulse force among nanoparticles. Intrinsic viscosity can be calculated by both Huggins' and Kraemer's equations, the intrinsic viscosity of cationic nanoparticles were shown in Figure 4.10. There is a sudden jump of intrinsic viscosity at 10% cationic degree. Below 10% cationic

degree, intrinsic viscosity of dispersion is from 0.5 to 1dL/g. When the cationic degree increased from 10 to 20%, intrinsic viscosity of the dispersion was increased from 1 to 5.3dL/g.

Huggins Eq.:

$$\frac{\eta_{sp}}{c} = [\eta] + k_H[\eta]^2c \quad (15)$$

Kraemer Eq.:

$$\frac{\ln \eta_r}{c} = [\eta] - k_K[\eta]^2c \quad (16)$$

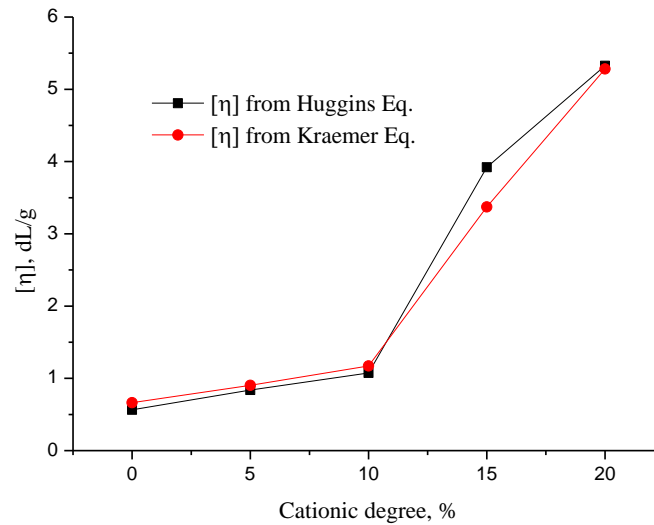


Figure 4.10. Intrinsic viscosity of cationic nanopartilces (● intrinsic viscosity by Kraemer Equation, ■ intrinsic viscosity by Huggins Equation).

Cationic charge on nanoparticle can increase electrostatic repulsion among nanoparticles. And as surface charge increases, repulse force first increases slightly. After cationic degree above 10%, dispersion viscosity has a significant increasing.

Polyacrylamide nanoparticle can hydrolyze as $-\text{CONH}_2$ groups turned into $-\text{COO}^-$ groups. Thus, provide negative charges on nanoparticle surface. When cationic degree below 10%, positive charge provided by cationic groups was neutralized by hydrolyzed amide groups.

4.3.3 Effect of Salinity on Nanoparticles. The charge valences of the ions in saline solution and salt concentration greatly influenced the swelling behavior of the cationic nanoparticles.

The swelling of the nanoparticles in saline solutions was appreciably decreased compared to the values measured in deionized water. This phenomenon was attributed to a charge screening effect of the additional ions causing a non-perfect electrostatic repulsion, leading to the decreased osmotic pressure (ionic pressure) difference between the hydrogel network and the external solution.

As shown in Figure 4.11, the nanoparticle's diameter decreased when brine concentration increased to 0.5wt.%, then the diameter kept constant as the salt concentration further increasing. According to Flory's equation, the effect of the ionic strength on the water absorbency can be expressed by:

$$Q^{\frac{5}{3}} = \frac{\left(\frac{i}{V_u}\right)^2 + \left(\frac{1}{2} - x_1\right)/V_1}{V_E/V_0} \quad (17)$$

where Q is the degree of swelling, i/V_u is the charge density of polymer, S is the ionic strength of solution, $(1/2 - x_1)/V_1$ is the polymer-solvent affinity, and V_E/V_0 is the crosslinking density.

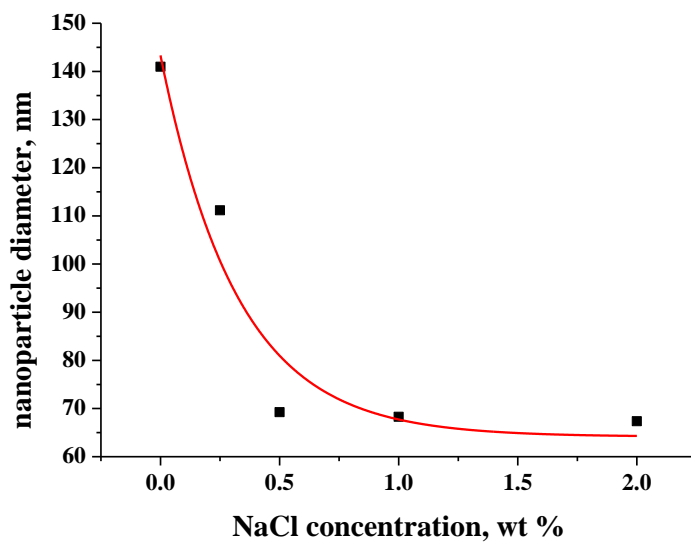


Figure 4.11. Measured equilibrium swelling diameter of cationic nanoparticle (15% cationic degree) in different brine solution.

The viscosity of nanoparticles dispersion was measured by Brookfield DV-III viscometer. The infinite shear viscosity versus brine concentration of dispersion was shown in Figure 4.12.

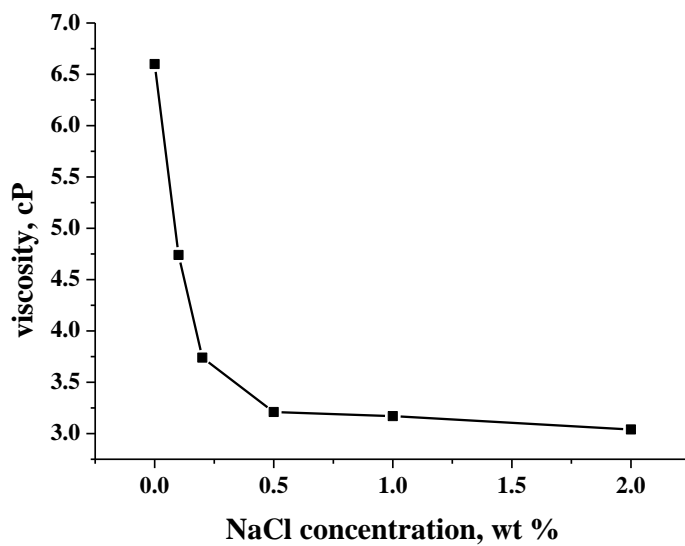


Figure 4.12. The infinite shear viscosity of nanoparticle dispersion.

Generally, the addition of salt to the dispersion system will cause viscosity increase. However, viscosity can be decreased as the particle size shrinks, leading to the decrease of the particle volume fraction as demonstrated in previous research. In our case, as salt concentration increased, the dispersion viscosity first decreased significantly (brine concentration 0 to 0.5wt.%) and then kept constant. Apparently, the viscosity of the dispersion system was dominated by the polymeric nanoparticle size. The larger and softer the nanoparticles were, the easier they would collide and lose energy. Thus, nanoparticle dispersion at low brine concentration was more viscous. When brine concentration beyond certain level, nanoparticle size and dispersion viscosity would not change with it.

Zeta-potential of nanoparticles dispersions with different salinity was shown in Figure 4.13. The Zeta-potential decreased from 43 to 5mV with the increase of salt

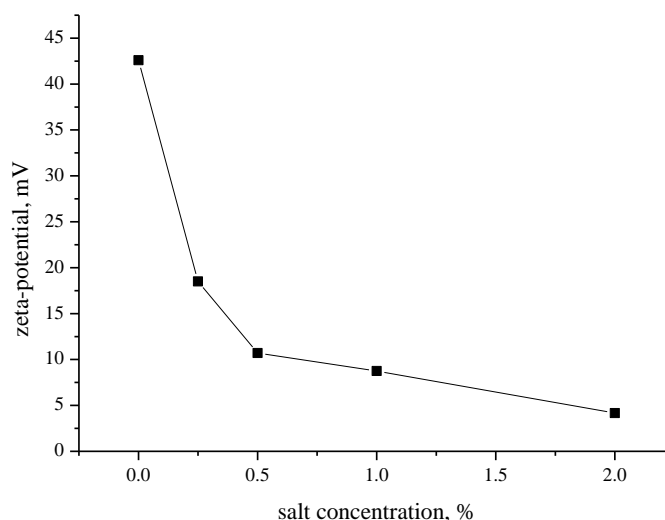


Figure 4.13. Zeta potential of 15% cationic degree nanoparticles as a function to the surrounding solution salt concentration (from 0 to 2%).

concentration from 0 to 2wt.%. Cation in nanoparticles can provide positive charge on particle's surface, and this positive charge was sensitive to Cl^- in salt solution. Zeta-potential measured potential besides stern layer.

Cl^- ions concentration was much higher than OH^- in salt solution, therefore Cl^- can absorb more between cationic nanoparticles' surface and stern layer than OH^- . Caused by more negative charge absorbed on cationic nanoparticles, potential besides slipping plane was decreased. And Zeta-potential was keeping decrease with Cl^- concentration increases.

4.3.4 Effect of PH on Nanoparticles. To investigate the influence of pH on the equilibrium swelling ratio of 15% cationic degree hydrogel, the pH range was selected from 1.0 to 7.0 in this study. The equilibrium swelling ratios of hydrogel under room temperature of different pH values were shown in Figure 4.14.

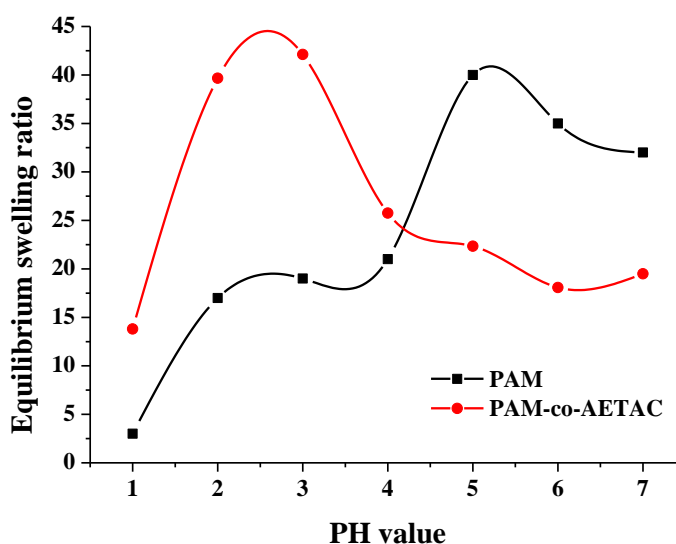


Figure 4.14. Equilibrium swelling ratio of 15% cationic degree hydrogel (PAM-co-AETAC) and PAM in different pH value solutions (from 1.0 to 7.0).

This cationic hydrogel has higher swelling ratio under acidic condition (2.0 to 4.0) than neutral, and when pH was lower than 2, this hydrogel turned to shrink. In the case of poly(AM-co-AETAC) hydrogel, which contains amine groups, the maximum degree of swelling of poly(AM-co-AETAC) hydrogel was attained at pH 2 to 3. The swelling was due to the complete protonation of amine groups at this pH value. With the hydrolysis of poly(AM-co-AETAC) hydrogel, some parts of amide groups were converted to carboxylate groups.

In Figure 4.14, PAM hydrogel had a swelling peak while pH value around 5. And when pH value was 2 to 4 PAM hydrogel equilibrium swelling ratio did not change too much.

For PAM hydrogel the species involved were $-\text{NH}_3^+$ (at acid conditions), $-\text{NH}_2$ (at neutral pH) and for poly(AM-co-AETAC) hydrogel the species were $-\text{N}(\text{CH}_3)_3^+$. Under acidic conditions, the swelling of PAM hydrogel was controlled mainly by the amino group on the carbon chains. It was a weak base group with pK_a of 6.5. Under the acidic conditions, it would get proton and increased charge density of polymer chains. Due to the electrostatic repulsion between $-\text{NH}_3^+$ groups, the osmotic pressure inside PAM hydrogel particles would increase. The osmotic pressure difference between internal and external solution was balanced by the swelling of PAM hydrogel. However, under strong acidic conditions, a screening effect of the counter ion took dominate, Cl^- shielded the charge of ammonium cation and prevents an efficient repulsion. As a result, an obvious decrease in equilibrium swelling ratio was observed when pH value turned from 2 to 1. And equilibrium swelling ratio did not show a significant alteration as balanced by electrostatic repulsion and screening effect.

For poly(AM-co-AETAC) hydrogel, $-\text{NH}_2$ turned to $-\text{NH}_3^+$, which increasing the electrostatic repulsion between $-\text{NH}_3^+$ and $-\text{N}(\text{CH}_3)_3^+$. Thus, the osmotic pressure inside poly(AM-co-AETAC) hydrogel would increase and hydrogel would swell more in low pH. In high pH value, quaternary N was hydroxylated, which means anion been removed and electrostatic repulsion was minimized, so that the hydrogel shrank as pH went from 4 to 7.

5 SIZE CONTROL OF NANOPARTICLES

5.1 MATERIALS

Acrylamide, 98+% (AM) and N-decane, 99% were from Alfa Aesar. N,N'-methylene bisacrylamide, 99% (MBAA), acetone, for HPLC $\geq 99\%$, docusate sodium (AOT), and Polyethylene glycol sorbitan monostearate, (Tween 60) were purchased from Sigma-Aldrich. Sorbitan monooleate, (Span 80) viscosity 1200-2000 mPa•s (20 °C) was from Fluka. Mineral oil (light), was from Fisher Chemical. Ammonium persulfate, BP179-100 (APS) was from Fisher bioreagent. Dodecyl sulfate, sodium salt, 98% was from Aldrich chemical. Water used in the following experiments was deionized (DI) water and all the chemicals were used as received.

5.2 DIFFERENT FACTORS EFFECT ON PARTICLE SIZE

Diameters of nanoparticle can be controlled by several factors: stirring rate, emulsifier concentration, and emulsifier type. Monomer concentration, initiator concentration, and number of portions also effected particle diameter. However, these three factors can affect gel properties, such as gel strength, as well. Hence, in this experiment, stirring rate, emulsifier concentration, and emulsifier type effect were studied.

The stability of emulsion and diameter of droplet were dominated by the structure of emulsifier. The structures of different surfactants were shown in Figure 5.1.

AOT and SDS are anionic surfactants; Tween60 and Span80 are nonionic surfactants. The structure of AOT was different from the structure of SDS. AOT had two

Table 5.1. HLB and CMC of different surfactants.

| Surfactant | HLB | CMC/ mmol/L |
|------------|------|-------------|
| Span80 | 4.3 | <5 |
| Tween60 | 14.9 | 28 |
| SDS | 40 | 8.6 |
| AOT | 10 | 5 |

Table 5.2. Experiments design of nanoparticle synthesis.

| Number | O: W: S/ g: g: g | Surfactant | 10wt.% initiator solution/ mL | Stirring rate/ rpm | Temperature/ °C |
|--------|---------------------|---------------------|-------------------------------------|-----------------------|-----------------|
| #1 SC | 4: 3: 3 | Span80 & Tween60 | 0.2 | 600 | 40 |
| #2 SC | 4: 3: 2.5 | Span80 & Tween60 | 0.2 | 600 | 40 |
| #3 SC | 4: 3: 2 | Span80 & Tween60 | 0.2 | 600 | 40 |
| #4 SC | 4: 3: 1.5 | Span80 & Tween60 | 0.2 | 600 | 40 |
| #5 SC | 4: 3: 1 | Span80 & Tween60 | 0.2 | 600 | 40 |
| #6 SC | 4: 3: 2.5 | Span80 & Tween60 | 0.2 | 500 | 40 |
| #7 SC | 4: 3: 2.5 | Span80 & Tween60 | 0.2 | 400 | 40 |
| #8 SC | 4: 3: 2.5 | Span80 & Tween60 | 0.2 | 700 | 40 |
| #9 SC | 4: 3: 2.5 | Span80 & Tween60 | 0.2 | 800 | 40 |
| #10 SC | 4: 3: 0.84 | SDS | 0.2 | 600 | 40 |
| #11 SC | 4: 3: 1.6 | AOT | 0.2 | 600 | 40 |

For #1 SC to #9 SC experiments, the emulsions before initiated were stable for several days or even several weeks. However, for #10 SC and #11 SC, the emulsions were not stable. Phase separation happened in few minutes for #11 SC. The photo of #10 emulsion was shown in Figure 5.2.

The polymerize result of #10 SC and #11 SC were shown in Figure 5.3 to Figure 5.4.



Figure 5.2. Water in oil emulsion stabilized by SDS.



Figure 5.3. Polymerization result of SDS stabilized emulsion.

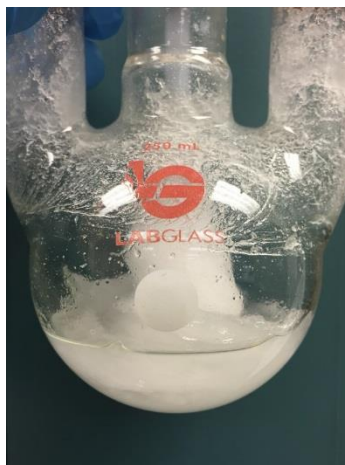


Figure 5.4. Polymerization result of AOT stabilized emulsion.



Figure 5.5. Product of #10 SC sample

The morphology of samples #1 SC to #9 SC was measured by scanning electron microscope (SEM). The samples preparation process was: washed nanoparticles out by acetone from the synthesis production; then, dispersed precipitates (nanoparticles) in acetone and removed supernatant liquid by ultracentrifuge (4000rpm), this procedure was circled for three times; white precipitates were collected and dried in vacuum oven under

60°C; finally, dried particles was paste on carbon-dots on the stub and crashed into even smaller powders before put into chamber.

The morphology was shown in Figure 5.6 – Figure 5.14.

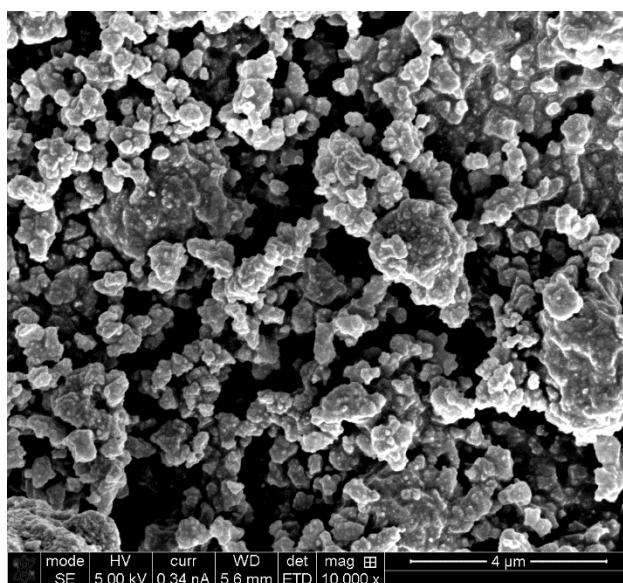


Figure 5.6. SEM photo of #1 SC.

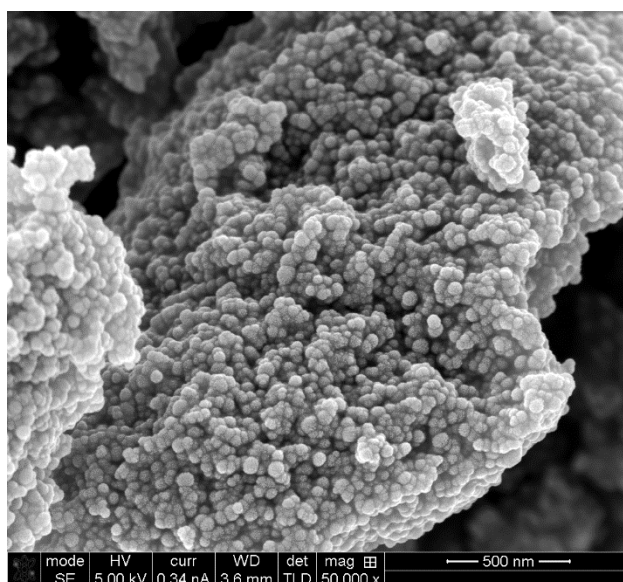


Figure 5.7. SEM photo of #2 SC.

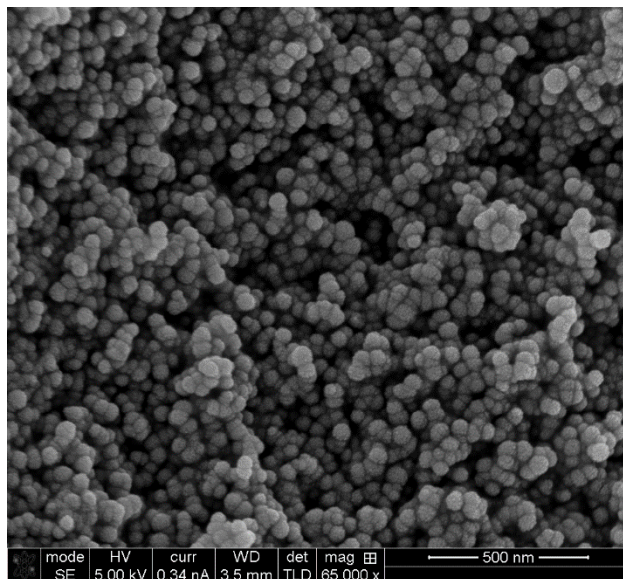


Figure 5.8. SEM photo of #3 SC.

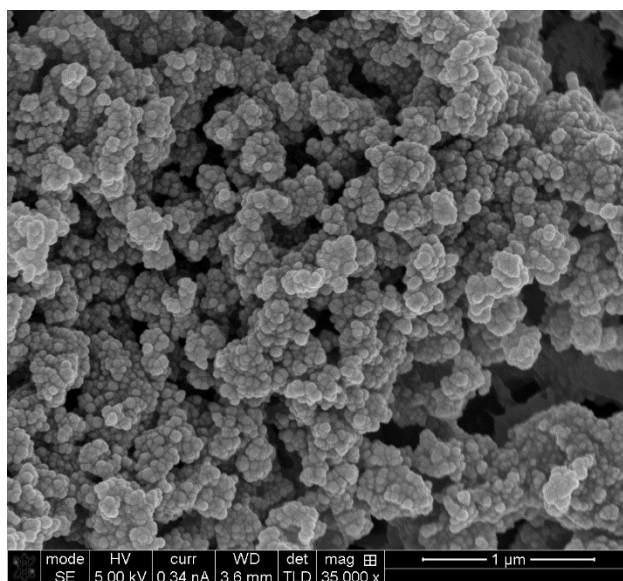


Figure 5.9. SEM photo of #4 SC.

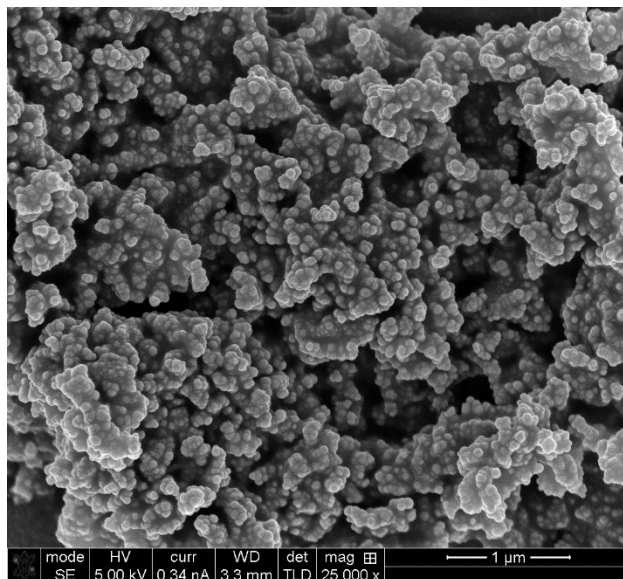


Figure 5.10. SEM photo of #5 SC.

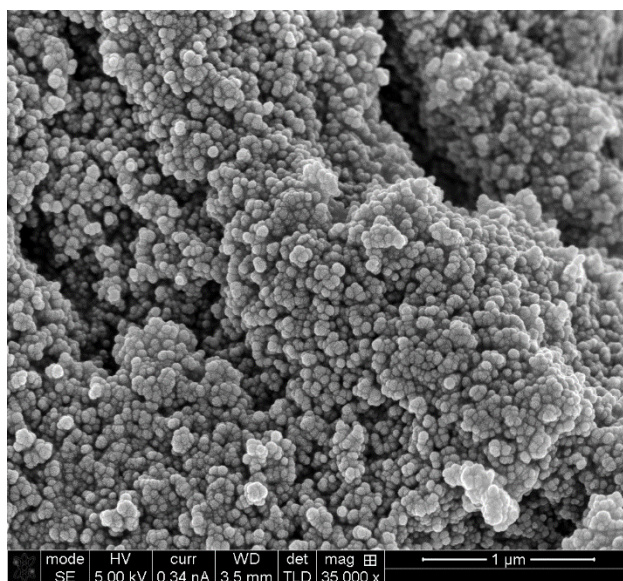


Figure 5.11. SEM photo of #6 SC.

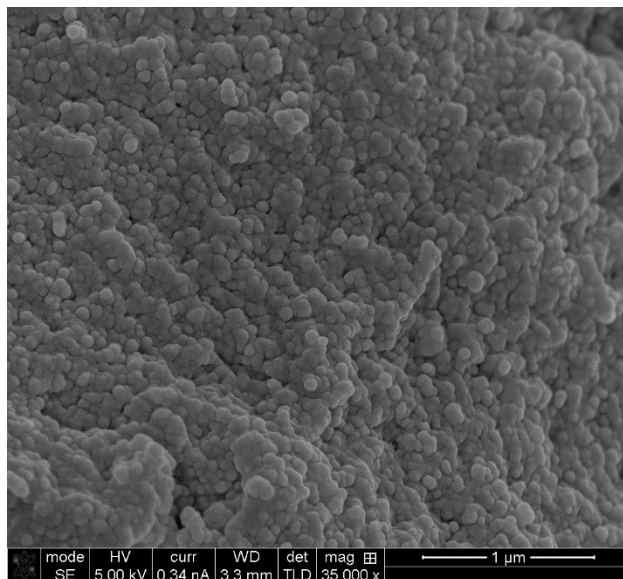


Figure 5.12. SEM photo of #7 SC.

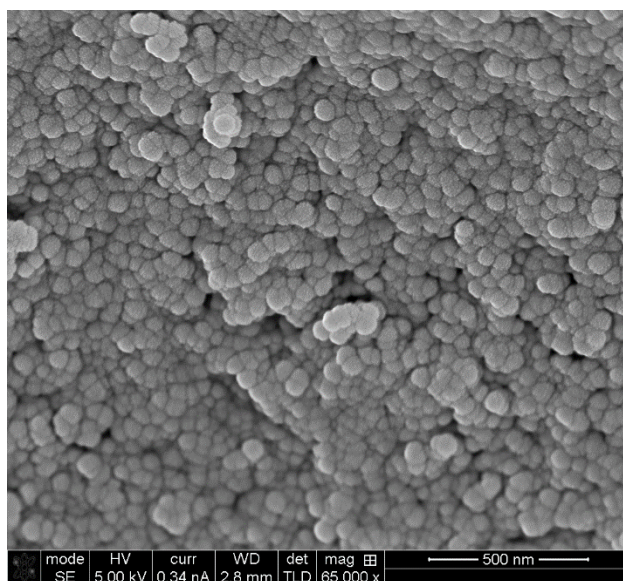


Figure 5.13. SEM photo of #8 SC.

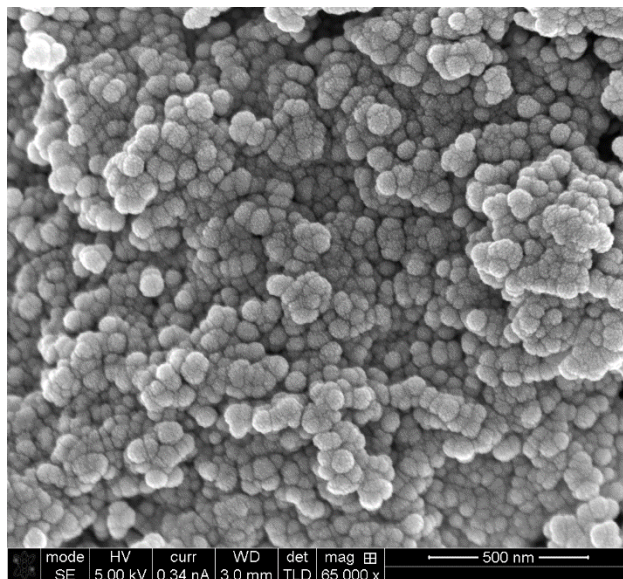


Figure 5.14. SEM photo of #9 SC.

Compare experiments from #1 SC to #11 SC, #10 SC and #11 SC samples formed bulk gels instead of nanoparticles by adding same molar amount of surfactant. SDS and AOT surfactants were widely used for suspension/ emulsion polymerization. However, HLB value of SDS or AOT was much larger the surfactants mixture of Span80 and Tween60. So only by adding same molar amount of SDS or AOT cannot form the same stability emulsion compared with surfactant mixture.

In #1 SC to #9 SC experiments, microemulsion can be formed by using the surfactants mixture. As surfactant concentration increasing, diameter of nanoparticles changed slight larger from #1 SC to #4 SC. However, diameter of #5 SC sample was much larger than #1 SC to #4 SC ones. By control surfactant concentration, diameter of nanoparticles can be controlled. What's more important, after choosing certain diameter of production, cost can be reduced by reducing surfactant amount in some range.

In #2 SC and #6 SC to #9 SC experiments, stirring rate was controlled. And the diameters of nanoparticles were almost the same, except #7 SC. In #7 SC experiment, stirring rate was 400rpm. And shear provided by 400rpm stirring was not high enough to prevent droplets collapsing during polymerization. This might be caused by: a) shear is not high enough to separate droplets after they collapsing with each other; b) the heat provided by polymerization cannot transfer very well and caused over heat to accelerate polymerization in some position. Diameters in #8 SC and #9 SC were slightly smaller compared with #2 SC and #6 SC. The higher stirring rate (in 400rpm to 800rpm range), the smaller particle diameter was.

Figure 5.15 showed the morphology of aggregations. The aggregation was caused

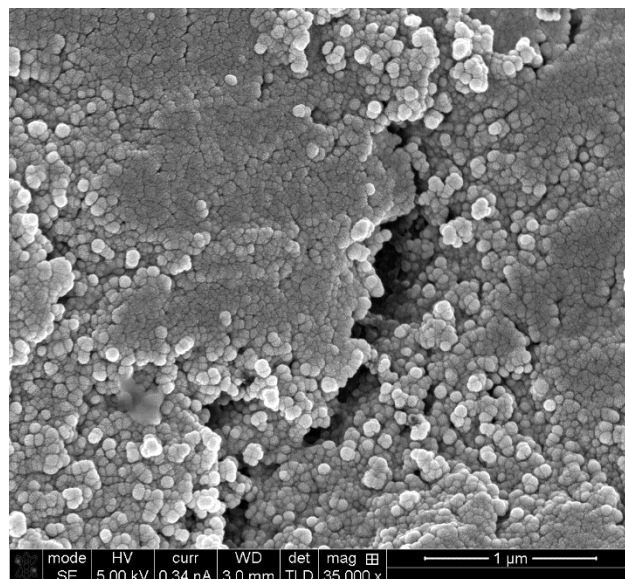


Figure 5.15. Flat surface of nanoparticles aggregation.

by ultracentrifuge during the purify process: a) PAM nanoparticles were hydrophilic and polar. After dropped into acetone, which was non polar solvent, nanoparticles were

aggregating with each other by like dissolves like; b) PAM nanoparticles were aggregated by several G (gravity) provided by ultracentrifuge.

However, the aggregation was easily breaking down. This can be proved by DLS result.

6 CONCLUSION

In this study, microemulsion was prepared by n-decane, aqueous solution and surfactants mixture. The boundary of emulsion and microemulsion was determined by both conductivity and light transmittance. The surfactants mixture of 70wt.% Span80 and 30wt.% Tween60 was the best one to prepare microemulsion in decane-water system.

Nanoparticles with different cationic degrees were synthesized via suspension polymerization. And morphology of cationic nanoparticles was measured by ESEM and SEM. Nanoparticles had larger surface charge (stern layer) with increased cationic degree. By introducing cationic groups into nanoparticles, nanoparticles can stand low pH and salt conditions.

Surfactant type, surfactant concentration, and stirring rate were evaluated for nanoparticle synthesis. SDS and AOT cannot form stable emulsion by just convert molar amount from surfactants mixture (Span80 & Tween60). Surfactant concentration did not affect the size of nanoparticles much after exceeding certain amount. Stirring rate is a key point for nanoparticle synthesis. Too low stirring rate can enlarge the change for dispersed droplets aggregate with each other, and increase the size and dispersity of product.

BIBLIOGRAPHY

Al-Anazi, H. A., & Sharma, M. M. (2002, January 1). Use of a pH Sensitive Polymer for Conformance Control. Society of Petroleum Engineers. doi:10.2118/73782-MS

Anderson R B. Schulz-Flory equation[J]. Journal of Catalysis, 1978, 55(1): 114-115.

Argentiere, Simona, et al. "A novel pH-responsive nanogel for the controlled uptake and release of hydrophobic and cationic solutes." *The Journal of Physical Chemistry C* 115.33 (2011): 16347-16353.

Atta, Ayman M., et al. "Novel dispersed magnetite core-shell nanogel polymers as corrosion inhibitors for carbon steel in acidic medium." *Corrosion science* 53.5 (2011): 1680-1689.

Bai, B., Shuler, P., Qu, Q., & Wu, Y. (2012). Preformed Particle Gel For Conformance Control. RPSEA Final Report, US DOE Contract, (07123-2).

Baker, J. P., Blanch, H. W., & Prausnitz, J. M. (1995). Swelling properties of acrylamide-based ampholytic hydrogels: comparison of experiment with theory. *Polymer*, 36(5), 1061-1069.

Batzilla, Thomas, and Werner Funke. "Formation of intra-and intermolecular crosslinks in the radical crosslinking of poly (4-vinylstyrene)." *Die Makromolekulare Chemie, Rapid Communications* 8.6 (1987): 261-268.

Chauveteau, G., Omari, A., Tabary, R., Renard, M., Veerapen, J., & Rose, J. (2001, January 1). New Size-Controlled Microgels for Oil Production. Society of Petroleum Engineers. doi:10.2118/64988-MS

Chauveteau, G., Tabary, R., Le Bon, C., Renard, M., Feng, Y., & Omari, A. (2003, January 1). In-Depth Permeability Control by Adsorption of Soft Size-Controlled Microgels. Society of Petroleum Engineers. doi:10.2118/82228-MS

Chauveteau, G., Tabary, R., Renard, M., & Omari, A. (1999, January 1). Controlling In-Situ Gelation of Polyacrylamides by Zirconium for Water Shutoff. Society of Petroleum Engineers. doi:10.2118/50752-MS

Chen, Yunhua, Nicholas Ballard, and Stefan AF Bon. "Moldable high internal phase emulsion hydrogel objects from non-covalently crosslinked poly (N-isopropylacrylamide) nanogel dispersions." *Chemical Communications* 49.15 (2013): 1524-1526.

Cheung S, Ng R, Frampton H, et al. A swelling polymer for in-depth profile modification: update on field applications[C]//SPE Applied Technology Workshop of "Chemical Methods of Reducing Water Production," San Antonio, Texas, USA. 2007: 4-6.

Clarke, Kimberly C., Simon N. Dunham, and L. Andrew Lyon. "Core/Shell Microgels Decouple the pH and Temperature Responsivities of Microgel Films." *Chemistry of Materials* 27.4 (2015): 1391-1396.

Contin, Andrea, et al. "Metal nanoparticles inside microgel/clay nanohybrids: Synthesis, characterization and catalytic efficiency in cross-coupling reactions." *Journal of colloid and interface science* 414 (2014): 41-45.

Cook, Joseph Patrick, and David Jason Riley. "pH induced swelling of PVP microgel particles—A first order phase transition?." *Journal of colloid and interface science* 370.1 (2012): 67-72.

Coste, J.-P., Liu, Y., Bai, B., LI, Y., Shen, P., Wang, Z., & Zhu, G. (2000, January 1). In-Depth Fluid Diversion by Pre-Gelled Particles. Laboratory Study and Pilot Testing. Society of Petroleum Engineers. doi:10.2118/59362-MS

Destribats, Mathieu, et al. "Impact of pNIPAM microgel size on its ability to stabilize Pickering emulsions." *Langmuir* 30.7 (2014): 1768-1777.

Fernandez-Nieves, A., et al. "Charge controlled swelling of microgel particles." *Macromolecules* 33.6 (2000): 2114-2118.

Frampton, H., Morgan, J. C., Cheung, S. K., Munson, L., Chang, K. T., & Williams, D. (2004, January 1). Development Of A Novel Waterflood Conformance Control System. Society of Petroleum Engineers. doi:10.2118/89391-MS

Gota, Chie, et al. "Hydrophilic fluorescent nanogel thermometer for intracellular thermometry." *Journal of the American Chemical Society* 131.8 (2009): 2766-2767.

Hasegawa, Urara, et al. "Nanogel-quantum dot hybrid nanoparticles for live cell imaging." *Biochemical and biophysical research communications* 331.4 (2005): 917-921.

Hayashi, Hisato, et al. "pH-sensitive nanogel possessing reactive PEG tethered chains on the surface." *Macromolecules* 37.14 (2004): 5389-5396.

Hong, Jun, et al. "Stabilization of α -chymotrypsin by covalent immobilization on amine-functionalized superparamagnetic nanogel." *Journal of biotechnology* 128.3 (2007): 597-605.

Hooper, H. H., Baker, J. P., Blanch, H. W., & Prausnitz, J. M. (1990). Swelling equilibria for positively ionized polyacrylamide hydrogels. *Macromolecules*, 23(4), 1096-1104.

Hoshino, Yu, et al. "Reversible absorption of CO₂ triggered by phase transition of amine-containing micro-and nanogel particles." *Journal of the American Chemical Society* 134.44 (2012): 18177-18180.

Hu, Jian, et al. "High fracture efficiency and stress concentration phenomenon for microgel-reinforced hydrogels based on double-network principle." *Macromolecules* 45.23 (2012): 9445-9451.

Huh, C., Choi, S. K., & Sharma, M. M. (2005, January 1). A Rheological Model for pH-Sensitive Ionic Polymer Solutions for Optimal Mobility Control Applications. Society of Petroleum Engineers. doi:10.2118/96914-MS

Huppertz, Thom, and Cornelis G. de Kruif. "Structure and stability of nanogel particles prepared by internal cross-linking of casein micelles." *International Dairy Journal* 18.5 (2008): 556-565.

Johnson, Kai CC, Francisco Mendez, and Michael J. Serpe. "Detecting solution pH changes using poly (N-isopropylacrylamide)-co-acrylic acid microgel-based etalon modified quartz crystal microbalances." *Analytica chimica acta* 739 (2012): 83-88.

Karbarz, Marcin, et al. "Preparation and characterization of microcomposite based on environmentally sensitive microgel and conducting polymer." 224th ECS Meeting (October 27–November 1, 2013). Ecs, 2013.

Kolmakov, German V., Krzysztof Matyjaszewski, and Anna C. Balazs. "Harnessing labile bonds between nanogel particles to create self-healing materials." *ACS nano* 3.4 (2009): 885-892.

Lee, J. H., & Lee, K. S. (2013). Performance of Gel Treatments in Reservoirs with Multiscale Heterogeneity. *Journal of Chemistry*, 2013.

Lv, F. F., Zheng, L. Q., & Tung, C. H. (2005). Phase behavior of the microemulsions and the stability of the chloramphenicol in the microemulsion-based ocular drug delivery system. *International journal of pharmaceutics*, 301(1), 237-246.

Ma, Shaohua, et al. "Fabrication of Microgel Particles with Complex Shape via Selective Polymerization of Aqueous Two-Phase Systems." *small* 8.15 (2012): 2356-2360.

Mehta, S. K., & Bala, K. (2000). Tween-based microemulsions: a percolation view. *Fluid Phase Equilibria*, 172(2), 197-209.

Meier, W., & Eicke, H. F. (1996). Electric, dielectric and Kerr effect investigations in water-in-oil microemulsions. *Current Opinion in Colloid & Interface Science*, 1(2), 279-286.

Molina, Maria, et al. "Stimuli-responsive nanogel composites and their application in nanomedicine." *Chemical Society Reviews* 44.17 (2015): 6161-6186.

Morimoto, Nobuyuki, et al. "Self-assembled pH-sensitive cholesteryl pullulan nanogel as a protein delivery vehicle." *Biomacromolecules* 14.1 (2012): 56-63.

Ogolo, N. A., Olafuyi, O. A., & Onyekonwu, M. O. (2012, January 1). Enhanced Oil Recovery Using Nanoparticles. Society of Petroleum Engineers. doi:10.2118/160847-MS

Oishi, Motoi, and Yukio Nagasaki. "Synthesis, characterization, and biomedical applications of core-shell-type stimuli-responsive nanogels—Nanogel composed of poly [2-(N, N-diethylamino) ethyl methacrylate] core and PEG tethered chains." *Reactive and Functional Polymers* 67.11 (2007): 1311-1329.

Ozawa, Yayoi, et al. "Self-Assembled Nanogel of Hydrophobized Dendritic Dextrin for Protein Delivery." *Macromolecular bioscience* 9.7 (2009): 694-701.

Paez Yanez, P. A., Mustoni, J. L., Frampton, H., Relling, M. F., Chang, K.-T., & Hopkinson, P. C. (2007, January 1). New Attempt in Improving Sweep Efficiency at the Mature Koluel Kaike and Piedra Clavada Waterflooding Projects of the S. Jorge Basin in Argentina. Society of Petroleum Engineers. doi:10.2118/107923-MS

Peyrelasse, J., & Boned, C. (1990). Conductivity, dielectric relaxation, and viscosity of ternary microemulsions: the role of the experimental path and the point of view of percolation theory. *Physical Review A*, 41(2), 938.

Pritchett, J., Frampton, H., Brinkman, J., Cheung, S., Morgan, J., Chang, K. T., ... Goodgame, J. (2003, January 1). Field Application of a New In-Depth Waterflood Conformance Improvement Tool. Society of Petroleum Engineers. doi:10.2118/84897-MS

Rodriguez Pin, E., Roberts, M., Yu, H., Huh, C., & Bryant, S. L. (2009, January 1). Enhanced Migration of Surface-Treated Nanoparticles in Sedimentary Rocks. Society of Petroleum Engineers. doi:10.2118/124418-MS

Rousseau, D., Chauveteau, G., Renard, M., Tabary, R., Zaitoun, A., Mallo, P., ... Omari, A. (2005, January 1). Rheology and Transport in Porous Media of New Water Shutoff / Conformance Control Microgels. Society of Petroleum Engineers. doi:10.2118/93254-MS

Ryoo, S., Rahmani, A. R., Yoon, K. Y., Prodanović, M., Kotsmar, C., Milner, T. E., ... & Huh, C. (2012). Theoretical and experimental investigation of the motion of multiphase fluids containing paramagnetic nanoparticles in porous media. *Journal of Petroleum Science and Engineering*, 81, 129-144.

Sahiner, Nurettin, et al. "Microgel, nanogel and hydrogel—hydrogel semi-IPN composites for biomedical applications: synthesis and characterization." *Colloid and Polymer Science* 284.10 (2006): 1121-1129.

Saunders, Brian R., and Brian Vincent. "Microgel particles as model colloids: theory, properties and applications." *Advances in colloid and interface science* 80.1 (1999): 1-25.

Schmidt, Sabrina, et al. "Influence of Microgel Architecture and Oil Polarity on Stabilization of Emulsions by Stimuli-Sensitive Core-Shell Poly (N-isopropylacrylamide-co-methacrylic acid) Microgels: Mickering versus Pickering Behavior?." *Langmuir* 27.16 (2011): 9801-9806.

Seiffert, Sebastian. "Small but Smart: Sensitive Microgel Capsules." *Angewandte Chemie International Edition* 52.44 (2013): 11462-11468.

Singka, Gillian S. Leslie, et al. "Enhanced topical delivery and anti-inflammatory activity of methotrexate from an activated nanogel." *European Journal of Pharmaceutics and Biopharmaceutics* 76.2 (2010): 275-281.

Sorrell, Courtney D., and Michael J. Serpe. "Reflection Order Selectivity of Color-Tunable Poly (N-isopropylacrylamide) Microgel Based Etalons." *Advanced materials* 23.35 (2011): 4088-4092.

Takahashi, Haruko, Shin-ichi Sawada, and Kazunari Akiyoshi. "Amphiphilic polysaccharide nanoballs: a new building block for nanogel biomedical engineering and artificial chaperones." *ACS nano* 5.1 (2010): 337-345.

Terashima, Takaya, et al. "Star-Polymer-Catalyzed Living Radical Polymerization: Microgel-Core Reaction Vessel by Tandem Catalyst Interchange." *Angewandte Chemie International Edition* 50.34 (2011): 7892-7895.

Thorne, Joanna B., George J. Vine, and Martin J. Snowden. "Microgel applications and commercial considerations." *Colloid and Polymer Science* 289.5-6 (2011): 625-646.

Van Poolen, H. K. (1980). *Fundamentals of enhanced oil recovery*.

Walsh, D., & Mann, S. (1996). Chemical synthesis of microskeletal calcium phosphate in bicontinuous microemulsions. *Chemistry of materials*, 8(8), 1944-1953.

Wang, Wenkai, et al. "Doubly crosslinked microgel-colloidosomes: a versatile method for pH-responsive capsule assembly using microgels as macro-crosslinkers." *Chemical Communications* 51.18 (2015): 3854-3857.

Weigert, S., Eicke, H. F., & Meier, W. (1997). Electric conductivity near the percolation transition of a nonionic water-in-oil microemulsion. *Physica A: Statistical Mechanics and its Applications*, 242(1), 95-103.

Wu, Weitai, et al. "A fluorescent responsive hybrid nanogel for closed-loop control of glucose." *Journal of diabetes science and technology* 6.4 (2012): 892-901.

Xiong, Meng-Hua, et al. "Lipase-sensitive polymeric triple-layered nanogel for "on-demand" drug delivery." *Journal of the American Chemical Society* 134.9 (2012): 4355-4362.

Xiong, Meng-Hua, et al. "Synthesis of PEG-armed and polyphosphoester core-cross-linked nanogel by one-step ring-opening polymerization." *Macromolecules* 42.4 (2009): 893-896.

Yan, Ming, et al. "Fabrication of single carbonic anhydrase nanogel against denaturation and aggregation at high temperature." *Biomacromolecules* 8.2 (2007): 560-565.

Yuan, You-Yong, et al. "Biocompatible and functionalizable polyphosphate nanogel with a branched structure." *Journal of Materials Chemistry* 22.18 (2012): 9322-9329.

Yunker, Peter J., et al. "Physics in ordered and disordered colloidal matter composed of poly (N-isopropylacrylamide) microgel particles." *Reports on Progress in Physics* 77.5 (2014): 056601.

Zaitoun, A., Tabary, R., Rousseau, D., Pichery, T. R., Nouyoux, S., Mallo, P., & Braun, O. (2007, January 1). Using Microgels to Shut Off Water in a Gas Storage Well. Society of Petroleum Engineers. doi:10.2118/106042-MS

Zhang, H., & Bai, B. (2010, January 1). Preformed Particle Gel Transport through Open Fractures and its Effect on Water Flow. Society of Petroleum Engineers. doi:10.2118/129908-MS

Zhang, T., Davidson, D., Bryant, S. L., & Huh, C. (2010, January 1). Nanoparticle-Stabilized Emulsions for Applications in Enhanced Oil Recovery. Society of Petroleum Engineers. doi:10.2118/129885-MS

VITA

Jiaming Geng received his Bachelor of Science degree in petroleum engineering from China University of Petroleum in June 2013. He joined Dr. Bai's group at Petroleum Engineering department in August 2013 as a graduate student in Missouri University of Science and Technology. In December 2015, he received his Master degree in Petroleum Engineering from Missouri University of Science and Technology.